Dan Shekwomwaza Solomon

Investigation of Production of Dimethyl Ether (DME) from Renewable Resources and its Integration into the Oil Production System

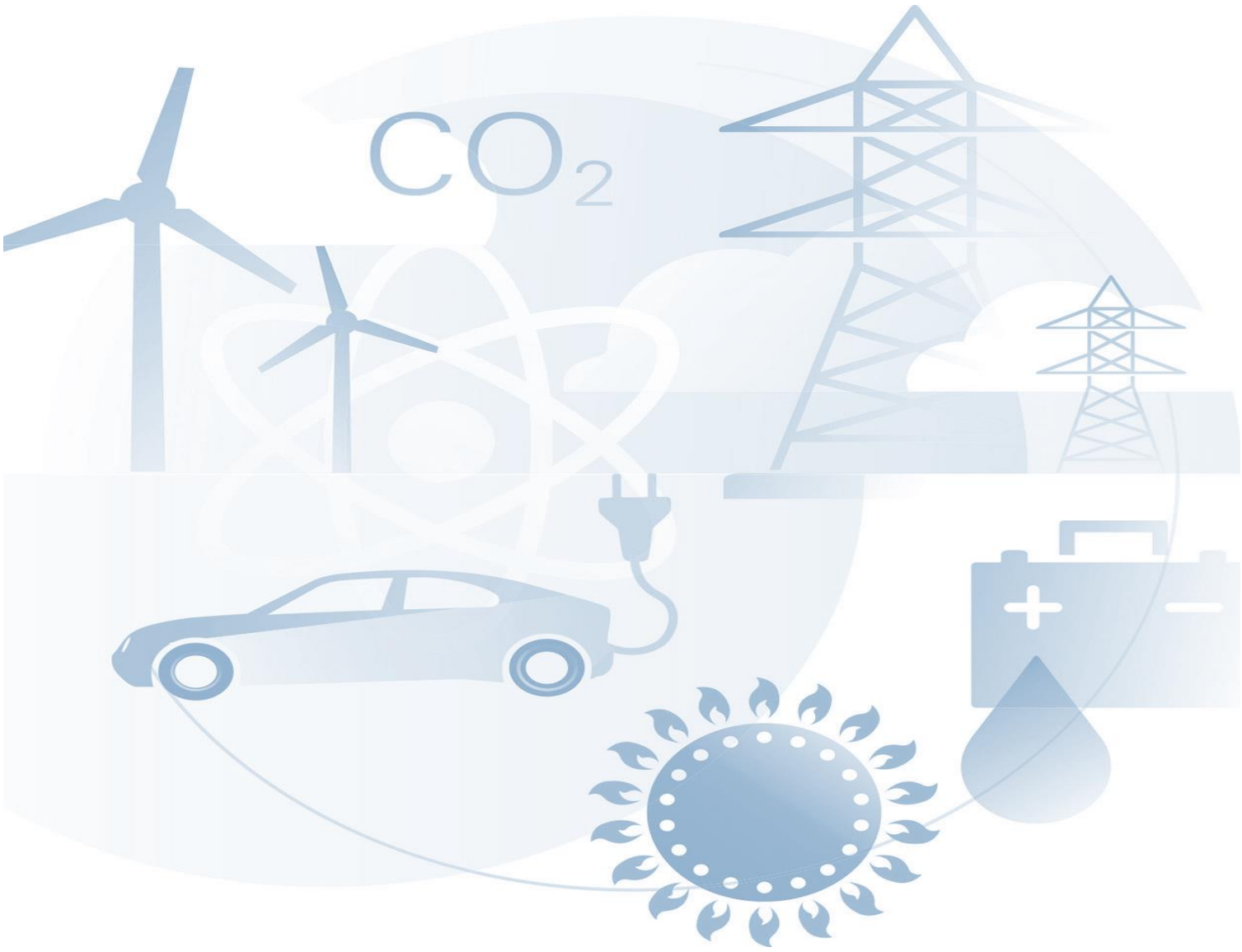

TU Delft Delft University of Technology

Page left intentionally blank

Investigation of Production of Dimethyl Ether (DME) from Renewable Resources and its Integration into the Oil Production System

By

Dan Shekwomwaza Solomon

in partial fulfilment of the requirements for the degree of

Master of Science

in Applied Earth Science

at the Delft University of Technology,

to be defended publicly on Tuesday December 19th, 2017

Supervisors:	Dr. Rouhi Farajzadeh	TU Delft
	Prof. Dr. Hans Bruining	TU Delft
Thesis Committee:	Prof. Dr. Bill Rossen	TU Delft
	Dr. Dennis Voskov	TU Delft
	Dr. Karl-Heinz Wolf	TU Delft

TU Delft

Page left intentionally blank

Abstract

Exergy investment in producing hydrocarbons is a relatively small fraction of the energy of the oil produced; yet it can reduce energy consumption in the order of percentages. In areas of high insolation or high wind speed, it can be considered that part of the exergy required for these purposes can be retrieved from sustainable energy sources. This idea is expected to be more important when applying enhanced oil recovery. As an example we use solvent (Dimethyl Ether - DME) enhanced water drive recovery. DME is a chemical solvent that has proven to be an efficient oil recovery agent. The recovered DME and oil are both considered products. The main invested exergy considered are the circulation costs of the fluids, separation/retrieval costs and the manufacturing costs of DME – it is assumed that DME is manufactured from natural gas using the single step direct method.

To improve the insight in the production process we develop a simple model of DME enriched brine injection in a 1-D reservoir. The model shows that about 92% of the oil in place is recovered using DME, which includes about 30% incremental production after water flooding. Moreover, 100% of the DME injected is recovered.

For the production /retrieval costs, we use a data set from the literature. The data set gives us the amount of DME /water injected and the amount of DME /oil/water produced. Moreover it gives the pressure drop, which allows us to calculate the power required for circulation of the fluids. Using these data, the exergy recovery factor (Ex_{RF}), which is defined as the exergy of the resources minus the exergy invested divided by the exergy of the resources produced (oil and DME) is calculated. It is observed that the Ex_{RF} initially increases with time before it declines and becomes negative. The time at which the Ex_{RF} becomes zero is called the exergy zero time. The result shows a negative exergy at the beginning of the DME enhanced water flood (DEW) process. As the incremental oil produced increases due to the presence of DME, and as more DME is back produced, which leads to less manufacturing of DME, the Ex_{RF} becomes positive. For DME enhanced recovery the initial area below exergy zero time plus the area above the exergy zero time is positive. Cumulatively, the result shows that at the end of the project, about 71% of the exergy is recovered.

The exergy analysis helps us to identify the various components that contribute the most to the exergy loss (~29%). DME manufacturing is found to be the most important contributor to the exergy loss, contributing ~80% (cumulative) to the total invested exergy. It shows that reducing the exergy of manufacturing DME increases the Ex_{RF}. The amount of DME lost in the reservoir is shown to also have an effect on the Ex_{RF} (not as much as the exergy of manufacturing DME), as it affects the utilization factor of DME. The utilization factor is the ratio of the oil produced (bbls) and the mass of DME injected. If DME is lost more DME must be injected without any increase in oil recovery and thus, DME loss reduces the Ex_{RF}.

CO_2 hydrogenation is chosen as one of the innovative ways of producing DME from renewable sources. The method utilizes CO_2 captured from burning the oil produced from the field in power plants and uses solar PV (photovoltaic) as the source of energy to produce H_2 from water electrolysis (see Eq. (1)).

$$2CO_2 + 6H_2 \rightarrow CH_3OCH_3 + 3H_2O. \quad (1)$$

The results show that the CO_2 captured from the power plant can be used to produce more DME than what is needed in the field. The excess DME can be reinjected or used for other purposes such as electricity generation, methanol production or for other uses e.g. as transportation fuel. It is also found that using CO_2 hydrogenation has the potential to reduce greenhouse gas emissions by about 82% compared to using natural gas for DME production, which means the method is cleaner and more sustainable.

Acknowledgement

First of all, I would like to thank God almighty for His grace and mercies and for the gift of life. Special thanks also go to my parents for their continuous support and perseverance over the years. God bless you. Now I can say I am coming home.

I would like to thank Dr. Rouhi Farajzadeh first of all for his innovative thinking in coming up with this topic and working hard to change the status quo in the oil and gas industry and secondly, for the continuous support during the course of the thesis. Your insights in this rather new area were very helpful. Special gratitude also goes to Prof. Dr. Hans Bruining, my daily supervisor. I really enjoyed working with you. Thank you for your patience and guidance throughout the course of the thesis and for being very critical of my work. I did learn a lot from working with you. It was a pleasure.

I would like to also thank the Justus & Louise van Effen foundation for offering me the scholarship to study at TU Delft. I would not have been able to study here if not for the scholarship. So thank you for making this dream a possibility.

Finally, I would like to thank all my friends for their continuous support and for always being there. God bless you.

Dan Shekwomwaza Solomon

Delft, December 2017

Table of Contents

Nomenclature

Greek Symbols

φ	Porosity
ρ_a	Aqueous phase molar density
ρ_o	Oleic phase molar density
ρ_{hex}	Density of hexadecane
ρ_w	Density of water
μ_a	Viscosity of the aqueous phase
μ_o	Viscosity of the oleic phase
μ_{dme}	Viscosity of pure DME
μ_w	Viscosity of water
μ_{hex}	Viscosity of hexadecane
η_{pump}	Pump mechanical efficiency
η_{driver}	Efficiency of electrical driver
η_{pp}	Efficiency of the power plant

Roman Symbols

D_{cap}	Capillary diffusion
D_m	Molecular diffusion
$Ex_{artificial\ lift}$	Exergy of artificial lift
Ex^{ch}	Chemical exergy
Ex^{ch}_{oil}	Chemical exergy of oil
Ex^{ch}_{psc}	Chemical exergy of the pseudo-components
$Ex_{Resource}$	Exergy of resources
$Ex_{invested}$	Invested exergy
Ex_{pump}	Pump exergy
f_w	Fractional flow of water
f_o	Fractional flow of water
g	Gravitational acceleration
ΔG_0	Standard Gibbs energies of formation
k_{rw}	Relative permeability of water
k_{ro}	Relative permeability of oil
${k_{rw}}^e$	End point permeability of water
${k_{ro}}^e$	End point permeability of oil
L	Length of reservoir
M_{hex}	Molar weight of hexadecane
M_{dme}	Molar weight of DME
M_{water}	Molar weight of water
n_w	Water saturation exponent
n_o	Oil saturation exponent
N_{pe}	Peclet number
PV	Pore volume
ΔP	Pressure difference
Pw_{pump}	Pump power requirement
$Pw_{gravity}$	Power saved due to gravity
$\dot{Q}$	Water injection rate
S_w	Water saturation

S_{wc}	Connate water saturation
S_o	Oil saturation
S_{or}	The residual oil
u	Darcy velocity
Vol_{a-dme}	Volume of DME in aqueous phase
Vol_w	Molar volume of water
Vol_{o-dme}	Volume of DME in the oleic phase
Vol_{hex}	Molar volume of hexadecane
V_{oil}	Volume of oil
V_{water}	Volume of water
V_{total}	Total volume
x_{da}	Mole fraction of DME in aqueous phase
x_{do}	Mole fraction of DME in oleic phase
x_{oa}	Mole fraction of oil in aqueous phase
x_{oo}	Mole fraction of oil in oleic phase
x_{wa}	Mole fraction of water in aqueous phase
x_{wo}	Mole fraction of water in oleic phase
x_i	Number of moles of the co-reactants / products

List of Abbreviations

ATR	Auto-thermal reforming
CCR	Carbon cycle recycling
CCS	Carbon capture and storage
CCU	Carbon capture and utilization
DEW	DME enhanced water flooding
DME	Dimethyl ether
EOR	Enhanced oil recovery
Ex_{RF}	Exergy recovery factor
LHV	Lower heating values
LLE	Liquid-liquid equilibrium
LPG	Liquefied petroleum gas
MTPD	Metric ton per day
PV	Pore volume
SG	Specific gravity
UNIFAC	UNIQUAC functional-groups activity coefficients
VOC	Volatile organic compound
WGS	Water gas shift

List of Figures

List of Tables

Page left intentionally blank

1 Introduction

Fossil fuels are major contributors of CO_2 emissions into the atmosphere. With the growing urge to keep global temperature rise below 2^{o} C, reducing these emissions into the atmosphere is considered of paramount importance. The dilemma; however, is the growth in the world's economy, which is expected to double in the next 20 years growing at about 3.4% per annum, with increase in productivity being one of the main drivers (BP, 2017). Moreover, the world's population is expected to reach about 8.8 billion people by 2025 with an increase in the number of middle class families (see Figure 1) (BP, 2017).

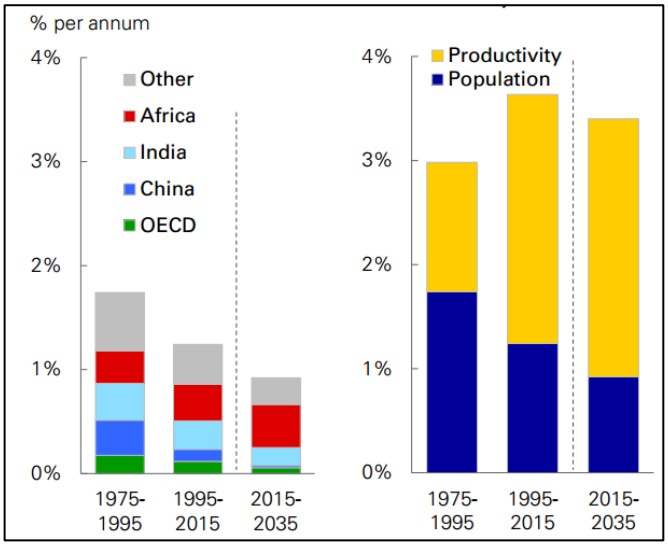

Figure 1 - Population Growth by Region (left) and Real GDP Growth by Factor (BP, 2017)

This growth especially in productivity and population would lead to more energy demand, which would in the short term mostly be met with fossil fuel as an energy source, at least for the foreseeable future (see Figure 2). This means that it is useful to develop innovative approaches that can be used to produce oil and gas with lower carbon footprints during this transition time and until "cleaner" renewable sources of energy are well established.

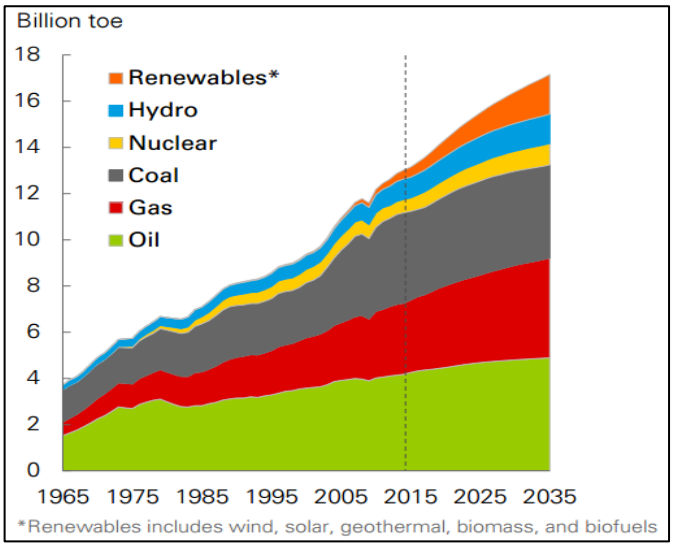

Figure 2 - Primary Energy Consumption by Fuel (BP, 2017)

This additional oil needed to meet the growing energy demands can be obtained using enhanced oil recovery (EOR). EOR is a tertiary recovery method used after primary (natural reservoir drive) and secondary (e.g. water flooding) recovery to reduce the residual oil saturation. It is very important because even after primary and secondary oil recovery, only about 50 to 55% of the oil originally in place (OOIP) is recovered for light oil, which means that the remaining oil can only be targeted using EOR (Thomas, 2008). EOR plays a more important role in heavy oil reservoirs, where about 90% of the OOIP can only be targeted using EOR (Thomas, 2008). The two main EOR techniques are thermal (e.g. steam ingestion or in situ combustion) and non-thermal (e.g. miscible flooding, chemical flooding, immiscible gas drives etc.). Over the years, chemical EOR methods such as surfactant and polymer flooding and other chemical EOR methods have gain increased applications. Recently, Shell developed a novel technology where Dimethyl Ether (DME), a chemical solvent is used for EOR. This solvent based EOR technique, which is a phase driven method can help to significantly increase oil recovery.

Two very important properties of DME make it a good candidate for enhanced water flooding. First, DME is soluble in water and it is first contact miscible with hydrocarbons (Chernetsky *et al.*, 2015). Due to its solubility, DME can be dissolved in water and injected into the reservoir through water injection. Upon contacting the fluids in the reservoir, DME immediately partitions into the trapped oil, leading to a reduction in viscosity and swelling of the oil. Due to this partitioning and reduction in viscosity, the mobility of the oil phase increases, making it easier to be displaced leading to an increase in recovery and a reduction in the remaining oil saturation (Chernetsky *et al.*, 2015; Parsons *et al.*, 2016).

1.1 Objectives of the Thesis

This thesis aims at developing sustainable methods of oil and gas production by utilizing renewable energy and other sustainable materials. The focus is on determining the sustainability of injecting Dimethyl Ether (DME) to produce oil.

The purpose of this work is on improving the understanding of exergy streams involved in solvent (DME) enhanced recovery. It uses an exergy balance model and estimates the exergy of various components involved in DME enhanced oil recovery. We use COMSOL to simulate the process to obtain the recovery profile.

1.2 Thesis Outline

The thesis starts by looking into DME and some of its properties that make it suitable for enhanced oil recovery. Furthermore, the various methods of commercially-producing the solvent are looked into in Chapter 2. Chapter 3 covers the DME Enhanced Water flood (DEW) method

by first understanding how the method works and the various factors affecting its effectiveness. This is followed by a simple 1-D simulation of the process using COMSOL in order to understand the physics of the process. Chapter 4 starts with a brief description of the exergy concept and its application to the DEW process. In the latter part of the chapter, an exergy analysis of the DEW process is carried out using data of a particular field from the literature. In Chapter 5, several methods of producing DME from renewables are investigated considering the feasibility, given the current state of the technologies. Finally, Chapter 6 concludes the thesis giving limitations of the work with recommendations for future work in Chapter 7.

2 Dimethyl Ether

Dimethyl Ether (DME) with chemical formula CH_3OCH_3 is the simplest ether. It is gaseous at ambient conditions and liquefies under moderate pressure with physical and chemical properties similar to that of liquefied petroleum gas (LPG) e.g. butane and propane (Semelsberger *et al.*, 2006). It has no direct C-C bond, but rather direct C-H and C-O bonds and contains about 35 wt.% oxygen (Azizi *et al.*, 2014). Owing to these properties, the combustion of DME releases no SOx, soots with less NOx emissions compared to Diesel (Taupy, 2007). Combining these features with its high cetane number (higher cetane number corresponds to shorter ignition delays), DME can be used as an alternative for fuel transportation (Azizi *et al.*, 2014). Table 1 highlights the physical properties of DME and propane.

Table 1 - Physical Properties of DME and Propane (te Riele et al., 2016)

Physical Properties	**DME**	**Propane**
Chemical formula	CH_3OCH_3	C_3H_8
Molecular weight (g/mol)	46.07	44.10
Lower heating value (MJ/kg)	28.43	46.4
Boiling point (^oC)	-24.8	-42.4
Critical Temperature (^oC)	126.9	96.8
Critical Pressure (bar)	53.7	42.6
Liquid density at 25^oC (kg/m^3)	668	509
Relative vapour density (sg.air)	1.63	1.55
Vapour pressure at 20^oC (bar)	5.10	8.33
Flash point (^oC)	-42.2	-104
Lower-Upper Explosive Limit (vol %)	2.7 - 32.0	1.7 - 10.8
Solubility in water at 20^oC (g/l)	70	0.075

Furthermore, though DME is a volatile organic compound (VOC), it is non-mutagenic, non-carcinogenic, non-teratogenic and non-toxic. This makes it a good aerosol propellant and refrigerant with zero potential to deplete the ozone layer (Semelsberger *et al.*, 2006). DME can also be used as polishing agent, pesticide, anti-rust agent, a source of hydrogen used in fuel cells, as well as important intermediate for producing key chemicals (e.g. light olefins, dimethyl sulphate etc.). Moreover, it has a great cooking and heating potential just like LPG since they exhibit similar properties. These similarities mean that DME can be transported and stored in existing LPG infrastructures (Semelsberger *et al.*, 2006). Table 2 summarizes some of the areas where DME fuel can be used as a substitute or as an additive to conventional fuel.

Table 2 - Fuel Usage by Sector (Inokoshi et al., 2005)

Sector	**Conventional Fuel**	**Synthetic Fuel**
Residential and Commercial	Coal, Kerosene, Natural gas, LPG	DME
Transportation	Gasoline, LPG, Diesel fuel	Methanol, Ethanol, CNG, DME
Power generation	Coal, heavy oil, Natural gas, LNG	DME, Methanol

Good *et al.* (1998) found that DME has a global warming potential of 0.3 (w.r.t. CO_2) averaged over 100 years compared to 21 in 100 years of methane (see Table 3). Evidently, DME has a lower global warming potential compared to carbon dioxide, methane and dinitrogen oxide. Based on this result, they concluded that DME is environmentally acceptable.

Table 3 - Global Warming Potential (Semelsberger et al., 2006)

	Time Horizon (Years)		
	20	100	500
DME	1.2	0.3	0.1
CO_2	1	1	1
CH_4	56	21	3.5
N_2O	280	310	170

The various properties listed above show that DME is a relatively clean energy source with great potential in the future. With a growing concern in climate change, oil supply and energy security, more adoption of DME in the future would play a central role in helping to solve these issues (Semelsberger *et al.*, 2006). This is part of what Olah *et al.* (2009) describes as the "Methanol Economy", since DME is a derivative of methanol.

In addition to the various usages of DME either as a fuel alternative or as an aerosol, Shell recently developed a novel technology where DME is used in enhanced water flood to help increase the oil recovery. At the moment, for this technology to be competitive with already existing technologies, DME has to be back produced and recycled due to the cost of the solvent. The cost of DME also plays a big role in the overall adoption as a fuel alternative. Therefore, DME has to be produced in large quantities to lower its cost. Currently, there are several industrial schemes for manufacturing DME. The most commonly-used scheme is the indirect production of DME from methanol: methanol dehydration to DME. Recently, there have been developments on the direct synthesis of DME from synthetic gas with the aim of producing it at a lower cost.

2.1 Current DME Industrial Scale Production Schemes

DME can be produced in two different ways using any methane containing feedstock e.g. natural gas, coal, oil, biomass etc. The first method which is the most popular at the moment is the indirect DME synthesis method. This method first converts the raw material (e.g. natural gas) to syngas (a mixture of hydrogen and carbon monoxide). In the presence of a catalyst, the syngas is converted to methanol – this is a very mature technology of methanol production. The obtained methanol is then dehydrated to get DME in the presence of another catalyst. The method is indirect because it is a two-step process involving first the production of methanol and then, DME. The second method is the direct DME synthesis method. Using this method, DME is produced from syngas directly without the intermediary step of methanol production. The method increases the conversion rate of syngas to DME better than what is obtained using the indirect method (The University of California, 2015). The DME cost is also lower using this method because of a simpler reactor design. This method, however, is more complex than the conventional indirect method making it, as yet, not suitable for commercial purposes (Azizi *et al.*, 2014). In recent years, however, there have been great progress towards making the method fit for commercial purposes. An example is the successful 100 ton/day commercial DME demonstration plant in Japan (Ogawa *et al.*, 2003). Figure 3 shows a schematic of both methods.

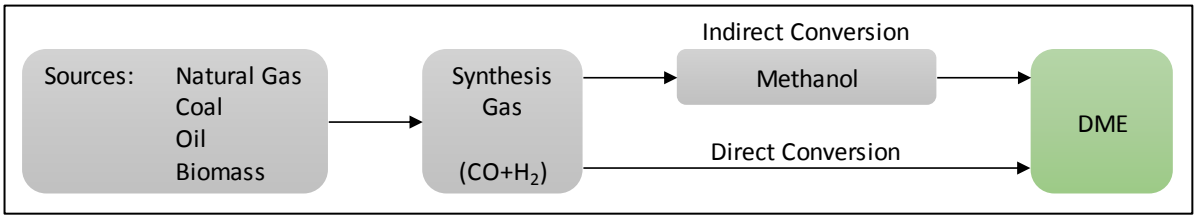

Figure 3 - DME Production (Azizi et al., 2014)

2.1.1 Indirect Synthesis Scheme

The reactions for the commercial production of DME are shown below. Eq. (2) shows the production of methanol from syngas and Eq. (3) the dehydration of methanol to DME.

$$2CO + 4H_2 \rightarrow 2CH_3OH, \quad (2)$$

$$2CH_3OH \rightarrow CH_3OCH_3 + H_2O. \quad (3)$$

Syngas is mainly produced from natural gas and coal. Using biomass as a feedstock is also becoming popular (Figure 3). Syngas production has a great impact on the price of methanol and thus, the price of DME. This is because generating the syngas accounts for more than 50% of the total investment in a methanol plant using natural gas as the raw material. This is higher for coal, where the investment for syngas generation accounts for 70-80% of total investment (Olah *et al.*, 2009).

2.1.1.1 Production from Natural Gas

Natural gas is one of the most widely used feedstock for methanol production (Kurniawan *et al.*, 2016). To get the desired DME, the DME plant can be integrated to a methanol plant close to a gas source for example. Another option is to have the methanol plant close to the gas source and then transport the produced methanol to a DME plant located close to a DME market (Kurniawan *et al.*, 2016). These two options are depicted in Figure 4. Other options are possible based on gas availability and the DME market.

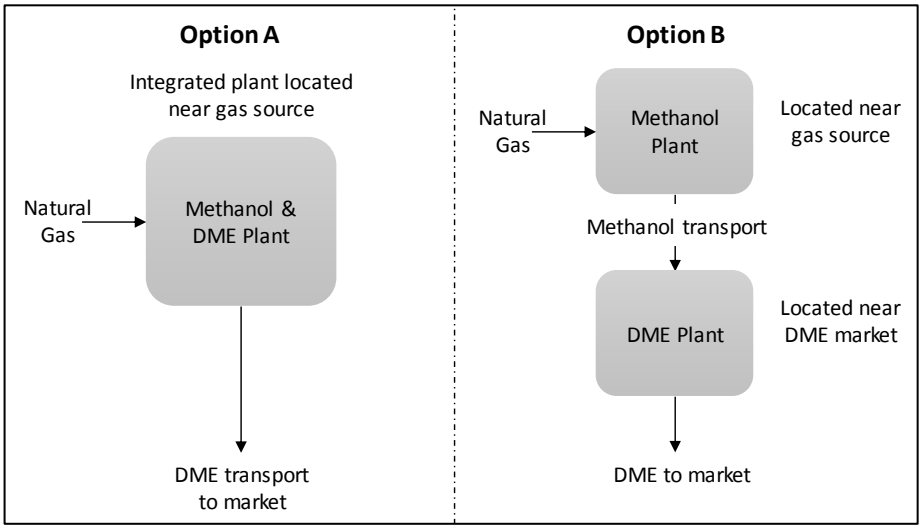

Figure 4 - Possible Options of DME Production from Natural Gas (Kurniawan et al., 2016)

Figure 5 shows the manufacturing process for both direct and indirect DME using natural gas.

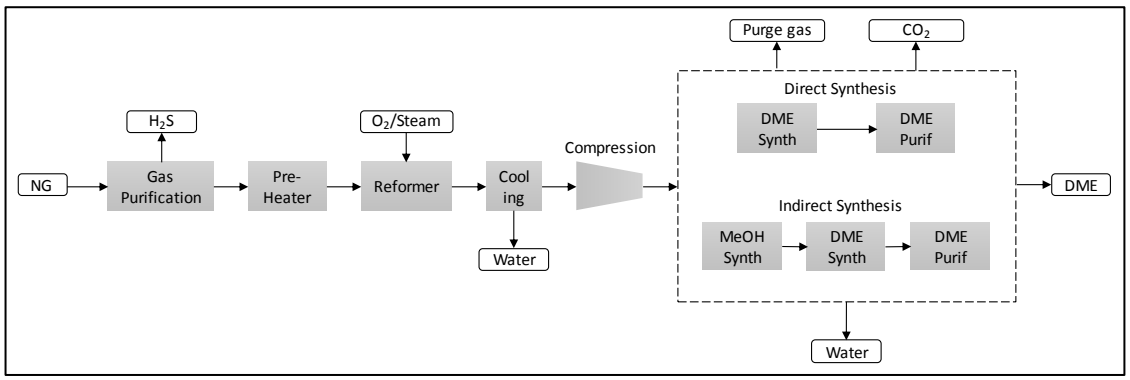

Figure 5 – Schematic Process Flow Diagram of DME Production from Natural Gas (Japan DME Forum, 2011)

There are several methods used to produce syngas from natural gas. These include: steam reforming, two step reforming, CO_2 reforming, auto-thermal reforming as well as partial oxidation of methane.

Steam Reforming

This refers to the steam reforming of methane. It is one of the most widely used methods for syngas production (te Riele *et al.*, 2016). The process involves heating methane with steam over a catalyst (e.g. nickel) at high temperature (typically 500 – 950^{o} C) and pressures between 20 and 40 bar (Roussière, 2013). The main products of the reaction are CO and H_2 (see Eq. (4)). A small amount of CO_2 is also formed in a water gas shift (WGS) as a result of CO reacting with steam (see Eq. (5)).

$$CH_4 + H_2O \leftrightarrow CO + 3H_2, \quad (4)$$

$$CO + H_2O \leftrightarrow CO_2 + H_2. \quad (5)$$

The amount of the components formed depends on temperature, pressure and the water/methane ratio (Olah *et al.*, 2009). Increasing the temperature and decreasing the pressure favours more CO and H_2 production because WGS reactions become less dominant leading to less CO_2 production. CO_2 production generally has an effect on the amount of DME produced (Azizi *et al.*, 2014). Typically, a high H_2/CO ratio (in this case, 3) would lead to less CO_2 production, and consequently less DME. Therefore, it is always desired to keep an optimum value for the H_2/CO ratio – about 2 for methanol synthesis (Japan DME Forum, 2011). One way of doing this is by adding CO_2 to the steam reformer's exit gas (Olah *et al.*, 2009).

Though one of the most widely-used methods, steam reforming is energy intensive making it a very expensive method. Another problem with steam reforming is the forming of soot or coke on the catalyst, the reformer as well as other equipment leading to clogging and hence, affects the efficiency of the whole process. This problem is; however, is solved by using excess steam (increases the cost) and shorter residence time in the reactor (Olah *et al.*, 2009).

Two Step Reforming

As the name implies, this method uses two steps to produce syngas. The first step converts about 35-45% of natural gas to syngas at relatively low temperature using the steam methane reforming process. A secondary reformer is then used to completely convert the natural gas to syngas using oxygen. Compared to the one step steam reforming process, the two step process can reduce the energy requirement by about 60% (Japan DME Forum, 2011).

Partial Oxidation of Methane

This involves reacting methane with insufficient oxygen with or without a catalyst (Olah *et al.*, 2009). The reaction is exothermic and is operated at higher temperatures (800-1500^{o} C) with pressures between 25 and 80 bar (Roussière, 2013). The H_2/CO ratio using this method is two (see Eq. (6)), which is good for methanol synthesis (Japan DME Forum, 2011; Olah *et al.*, 2009).

$$CH_4 + 0.5O_2 \leftrightarrow CO + 2H_2. \quad (6)$$

Due to the high temperatures, additional heat management equipment is needed. This combined with the cost of pure oxygen at high pressure increases the cost of this method (Roussière, 2013). Another problem related to using this method is that the syngas produced (CO and H_2) can be oxidized to form CO_2 and water producing excess heat, which is highly undesirable (Olah *et al.*, 2009).

Auto-Thermal Reforming (ATR)

This method combines steam reforming and the partial oxidation of methane to create a thermodynamically neutral reaction. This is possible because steam reforming is endothermic, while partial oxidation is exothermic and is usually operated at temperatures between (900 – 1500^{o} C) and pressures between 1 and 80 bar (Liu *et al.*, 2010). The obtained syngas using this method has a H_2/CO ratio close to two – suitable for methanol synthesis (Olah *et al.*, 2009). This process is very attractive because of the flexibility in the composition of the feedstock that can be used as well as the operating conditions (e.g. pressure) (Roussière, 2013). Though the method is still dependent of pure oxygen, which is expensive, ATR is most preferred for safe large scale and economic projects (Aasberg-Petersen *et al.*, 2003). ATR can be used as a

standalone technology or can be combined with a steam methane reforming known as combined reforming (see Appendix A for a typical ATR reactor).

Below are some usage of syngas technologies (from Air Liquide Engineering and construction) based on methanol plant capacities (Air Liquide, n.d):

- Conventional steam methane reforming – for small and medium sized methanol plants with capacity of up to 3000 MTPD (metric ton per day);
- Combined reforming – combines auto thermal reforming and steam reforming used for methanol plants with a capacity between 2,500 and 7,000 MTPD;
- ATR – used for methanol plants with a capacity above 7,000 MTPD and when the feedstock is light natural gas.

CO_2 Reforming of Methane

CO_2 reforming also known as dry reforming since it does not involve any steam is another method used to produce syngas. The method involves the reaction of CO_2 with methane. The reaction is endothermic (more than steam reforming) and is carried out over a catalyst, usually nickel based and temperatures between 800 and 1000^{o}C (Olah *et al.*, 2009).

$$CO_2 + CH_4 \leftrightarrow 2CO + 2H_2. \quad (7)$$

The advantage of using this method is that it can be very cost effective as well as environmentally acceptable if the heat needed for the reaction comes from renewable energies and the CO_2 is obtained from a rich stream such as industrial plants exhaust or captured from the atmosphere. Moreover, using this process, separating CO_2 from natural gas can be avoided, hence lowering the cost of purification (Goeppert *et al.*, 2014).

On the other hand, the H_2/CO ratio is one (see Eq. (7)). Though this is optimum for the direct DME synthesis, it is a disadvantage for methanol synthesis (Azizi *et al.*, 2014; Olah *et al.*, 2009). To help to remedy this, hydrogen from other sources would have to be added to the produced syngas, which is costly and increases the complexity of the process (Goeppert *et al.*, 2014; Olah *et al.*, 2009). Another disadvantage of the process is the carbon formation, which can shorten the catalyst lifetime.

Once the syngas has been obtained using any of the methods described above, methanol is produced and dehydrated to produce DME.

DME Synthesis from Methanol

The next step after syngas production is methanol synthesis. As mentioned earlier, conversion of syngas to methanol is a mature technology that is already being used for methanol production. The next step is then DME synthesis. Methanol is dehydrated at low temperature (exothermic reaction) to form DME. An example of a commercial scheme developed by TOYO Engineering Corporation for DME production using the indirect synthesis method is shown in Appendix B.

2.1.1.2 Production from Coal

DME can also be produced from coal. This method of production is very popular in China, where there are large coal deposits and producing a clean fuel such as DME from coal can play a big role in meeting the country's energy needs with minimal negative impact on the environment (Japan DME Forum, 2011). Similar to using natural gas, coal has to be first converted to syngas and then to methanol. Coal gasification is used to produce syngas from coal. There are different coal gasification designs, which are mainly dependent on the type of coal being used (Olah *et al.*, 2009). The gasification process combines partial oxidation and steam treatment. The equations below illustrates the process (Olah *et al.*, 2009) i.e.:

$$C + 0.5O_2 \leftrightarrow CO, \quad (8)$$

$$C + H_2O \leftrightarrow CO + H_2, \quad (9)$$

$$CO + H_2O \leftrightarrow CO_2 + H_2, \quad (10)$$

$$CO_2 + C \leftrightarrow 2CO. \quad (11)$$

Eqs. (8), (9), (10) and (11) show the different reactions in the coal gasification process. The process involves first coal gasification, followed by coal purification. After this step, the composition of the gas is adjusted to the desired composition for methanol synthesis. The H_2/CO ratio of coal is lower than one (typically between 0.5 and 0.7), which is not desired for methanol synthesis. This is because the syngas is usually rich in CO and CO_2 with a little amount of hydrogen. Therefore, to increase the amount of hydrogen, the syngas is subjected to a WGS reaction. The produced CO_2 is removed to the required level suitable for DME synthesis (Japan DME Forum, 2011). H_2S is also removed to prevent poisoning of catalysts (Olah *et al.*, 2009). Figure 6 shows the whole process for both direct and indirect DME synthesis.

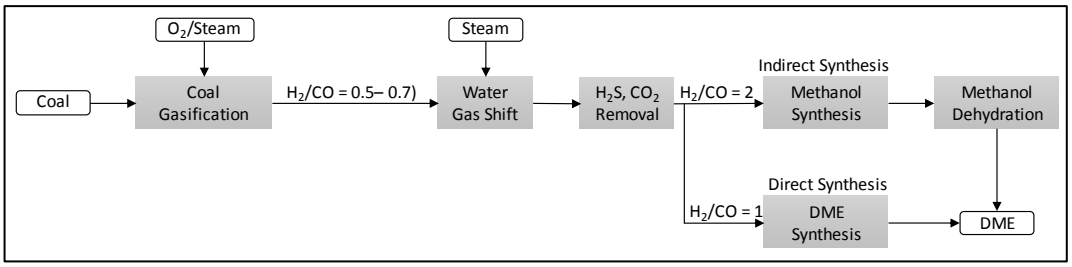

Figure 6 - Schematic Process Flow Diagram of DME Production from Coal (Japan DME Forum, 2011)

2.1.1.3 Production from Biomass

Another feed stock that is used for DME production is biomass. Just like the other feed stocks, biomass is first converted to syngas. The process flow of converting biomass to DME is similar to that of coal. However, due to the nature of biomass, it is first pre-treated. The next steps include gas purification, gas composition adjustment (gas reforming), methanol synthesis and thereafter DME synthesis. There have been several experiments on the feasibility of this method. However, there is no commercial or industrial scale plant yet using this method for DME production except for the pilot plant in Sweden – BioDME project (BioDME, n.d.). See (Japan DME Forum, 2011; Olah *et al.*, 2009; Santos *et al.*, 2015) for a detail description of the process.

2.1.2 Direct Synthesis Scheme

The second method for DME production is the direct synthesis method. In this case, DME is directly produced from syngas without the intermediary methanol production stage. As mentioned earlier, for DME to be competitive either as a fuel alternative or as an enhanced oil recovery agent, it should be produced in large quantities and at a low cost. The direct DME synthesis method is one of the ways this can be achieved. It is also more efficient to directly produce DME from syngas than to go through the methanol production phase (Ohno *et al.*, 2005). The method for syngas production is similar to those already described in sections above e.g. using the auto-thermal reforming (ATR) or steam reforming method. Eq. (12) shows the simple reaction of the direct synthesis method.

$$3CO + 3H_2 \rightarrow CH_3OCH_3 + CO_2. \quad (12)$$

As can be seen in Eq. (12), the optimum H_2/CO ratio using the direct synthesis method is one. Similar to the methanol synthesis case, the H_2/CO ratio affects the syngas conversion rate. In this case, a higher H_2/CO ratio reduces the DME selectivity and productivity.

Process Description

The direct synthesis method combines the methanol synthesis and dehydration process in a single reactor using a dual functional catalyst (allows both reaction in a single reactor) – typically Cu-based for methanol synthesis and an acidic catalyst for the dehydration step (Dadgar *et al.*, 2016). The conversion follows two main routes: the first is shown in Eq. (12) above and the second route in Eq. (13) below.

$$2CO + 4H_2 \rightarrow CH_3OCH_3 + H_2O. \quad (13)$$

The first route, which takes into account the water gas shift (WGS) reaction, synthesizes DME in three steps: methanol synthesis (see Eq. (14)), WGS reaction (see Eq. (15)) and methanol dehydration (see Eq. (16)), while the second route combines methanol synthesis (see Eq. (14)) and methanol dehydration (see Eq. (16)).

$$CO + 2H_2 \rightarrow CH_3OH, \quad (14)$$

$$CO + H_2O \rightarrow H_2 + CO_2, \quad (15)$$

$$2CH_3OH \rightarrow CH_3OCH_3 + H_2O. \quad (16)$$

CO_2 is the main by-product of Eq. (12), which is easier to separate from DME and also less energy intensive compared to separating water from DME – the main by-product of Eq. (13) (Inokoshi *et al.*, 2005). Another advantage of using Eq. (12) is the WGS reaction. Water accumulation in the reactor is undesirable as it leads to catalyst degradation. The WGS simultaneously converts water, which effectively helps to avoid water accumulation (Ogawa *et al.*, 2003). Using this route also allows higher conversion of syngas to DME (Olah *et al.*, 2009). Therefore, in general, Eq. (12) is used as the most preferred route in commercial direct synthesis DME plants. The JFE Corporation successfully used this route in their commercial demonstration plant of 100 ton/day in Japan.

The Reaction route shown in Eq. (12) is highly exothermic, which is why it is very important to control the temperature of the reaction because the DME catalyst used can gradually deactivate at high temperatures – typically over 300° C (Inokoshi *et al.*, 2005; Ogawa *et al.*, 2003). A slurry DME reactor is used to remedy this problem (see Appendix C for a concept of a slurry phase reactor).

The DME slurry reactor in combination with fine catalysts in the reactor helps to keep the temperature at a desired level. In the case where natural gas is used as the feed stock, an ATR reactor is used to obtain a H_2/CO ratio of one. Figure 7 shows the commercial scale of the direct DME synthesis process.

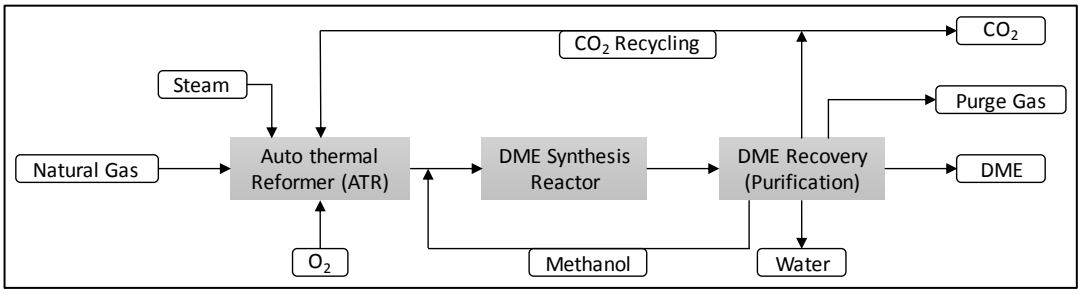

Figure 7 – Flow Diagram of DME Direct Synthesis Process (Japan DME Forum, 2011)

From Figure 7, most of the CO_2 produced is recycled and used in the ATR together with O_2 and steam to get the desired H_2/CO ratio of one (see Eq. (17)) (Inokoshi *et al.*, 2005).

$$2CH_4 + O_2 + CO_2 \rightarrow 3CO + 3H_2 + H_2O. \quad (17)$$

Another advantage of using this method is that it can utilize natural gas with a high CO_2 content of up to 40% without need for pre-treatment (Japan DME Forum, 2011). See Appendix D for the process flow of the JFE Corporation's commercial demonstration plant of 100 ton/day using the direct synthesis method.

In the case of a very high CO_2 content (> 40%), the CO_2 reforming (dry reforming) method can be used. As discussed earlier, this method produces syngas with H_2/CO ratio of one. Therefore, it can be used with DME synthesis using the first route described above. The reactions using this method are shown in Eqs. (18) and (19) (Olah *et al.*, 2009) i.e.:

$$3CH_4 + 3CO_2 \rightarrow 6CO + 6H_2, \quad (18)$$

$$6CO + 6H_2 \rightarrow 2CH_3OCH_3 + 2CO_2. \quad (19)$$

Coal can also be used as a feedstock instead of natural gas since by using coal, the H_2/CO ratio is almost close to one. The process works similar to that of indirect DME synthesis. The syngas H_2/CO ratio is adjusted to one in order to meet the requirement for direct DME synthesis. As is shown in Figure 8, the first step involves coal gasification with dry feeding. This is followed by a shift reaction. After this stage, CO_2 and H_2S are removed before DME synthesis. Following DME synthesis is the purification stage where the CO_2 obtained is used as a carrier gas. The CO_2 emitted can be captured and stored underground without needing any further separation due to the high purity (~99%) of the CO_2 obtained from the separation process (Japan DME Forum, 2011).

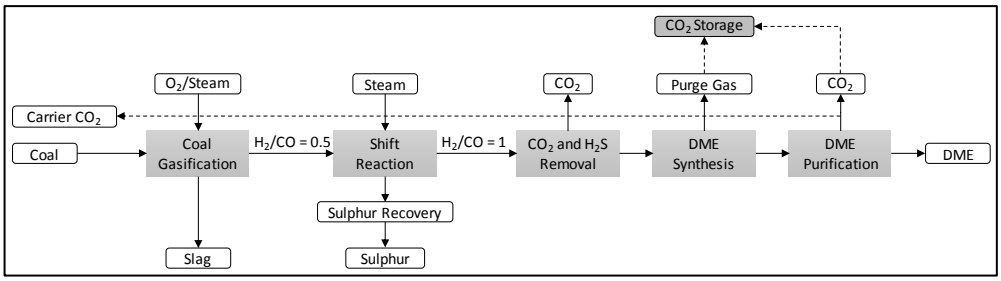

Figure 8 - Direct DME Synthesis Process from Coal (Japan DME Forum, 2011)

2.2 New and Innovative DME Production Methods

In the previous section, two main methods of DME production are discussed. These methods primarily use natural gas or coal as feed stocks for the production of syngas, which is then used to produce DME. Syngas generation is very energy intensive and is one of the most expensive parts in the overall production process. Therefore, eliminating this step would result in simplifying the process as well as substantially reducing the overall cost (Goeppert *et al.*, 2014). There are several new and innovative methods that have been developed or are being developed to help in this regards. Most of these methods revolve around the concept of carbon capture and recycling as well as the incorporation of renewable energies in the overall system to help improve the carbon footprint. Figure 9 shows the Carbon Cycle Recycling (CCR) concept for methanol and DME production as described in the "Methanol Economy" (Olah *et al.*, 2009).

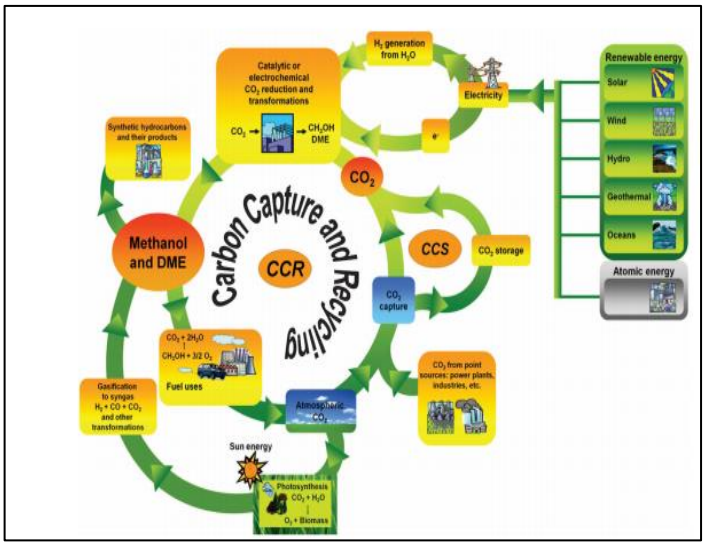

Figure 9 - Carbon Cycle and Recycling (Goeppert et al., 2014)

2.2.1 Hydrogenation of CO_2

Hydrogenation of CO_2 is an innovative method that has been developed for the production of methanol from CO_2 hydrogenation using either a homogenous or heterogeneous catalyst (Olah, 2013). The hydrogen needed for the reaction can be obtained from water electrolysis using renewable energy and the CO_2 used can be obtained from the exhausts of industrial plants (cement plants, power plants etc.) or natural sources such as CO_2 in natural gas or from geothermal wells (Olah, 2013). In addition to these, CO_2 could also be captured from the atmosphere (Olah, 2013). Eq. (20) below shows the reaction:

$$CO_2 + 3H_2 \rightarrow CH_3OH + 2H_2O. \quad (20)$$

The methanol obtained in this process can then be dehydrated to get DME (indirect DME synthesis). This method of methanol production is already being implemented in Iceland (see (The Ministry of industry *et al.*, 2010) for details of the project) and Japan with commercial demonstration plants (Goeppert *et al.*, 2014; Olah, 2013).

Similar to producing DME from syngas using the direct route, DME can also be produced directly through direct catalytic CO_2 hydrogenation (Olah *et al.*, 2009). The method works by using hybrid catalysts. The catalyst consists of both methanol synthesis and dehydration catalysts, which make it possible to directly obtain DME without going through the intermediary step of methanol production (Olah *et al.*, 2009). Eqs. (21) and (22) show the reactions involved in direct catalytic hydrogenation of CO_2.

$$2CO_2 + 6H_2 \rightarrow 2CH_3OH + 2H_2O, \quad (21)$$

$$2CH_3OH \rightarrow CH_3OCH_3 + 2H_2O. \quad (22)$$

Combining Eqs. (21) and (22) give a net reaction given in Eq. (23) below.

$$2CO_2 + 6H_2 \rightarrow CH_3OCH_3 + 3H_2O. \quad (23)$$

Figure 10 shows a flow diagram for the direct conversion to DME using renewable energy.

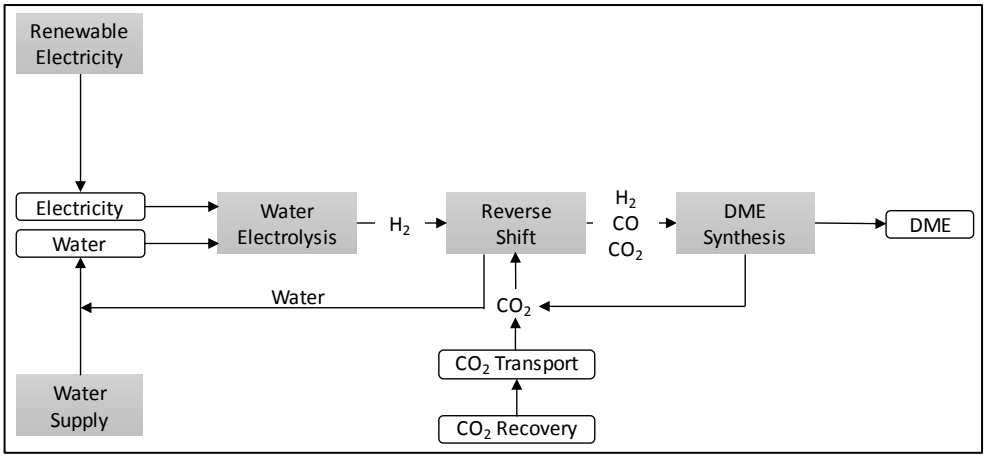

Figure 10 - Flow Diagram of CO_2 Hydrogenation using Renewable Energy (Japan DME Forum, 2011)

Other new technologies that are being developed for methanol (DME) production include the electrochemical CO_2 reduction to methanol and direct photochemical CO_2 reduction to methanol In addition to these, efforts have been made to produce methanol from methane without syngas production, with the aim of reducing the cost of production. Some of the methods being developed include: direct oxidation of methane to methanol, catalytic gas-phase oxidation of methane, liquid phase oxidation of methane, and methane conversion to methanol through monohalogenated methane See (Olah *et al.*, 2009) for detail description of these methods.

3 DME Enhanced Water-flood

DME enhanced water-flood (DEW) is a novel chemical EOR method developed by Shell. This solvent based EOR technique, which is a phase driven method can help to significantly increase oil recovery. Though only few papers have been published on this novel technology mostly from Shell, its application and effects on oil recovery is in line with earlier works that have been carried out over the past decades with regards to the use of miscible solvents to improve oil recovery (Gatlin and Slobod, 1960; Holm and Csaszar, 1962; Taber *et al.*, 1961; Taber and Meyer, 1964).

Two very important properties of DME make it a good candidate for enhanced water flooding. First, DME is soluble in water and it is first contact miscible with hydrocarbons (Chernetsky *et al.*, 2015). Due to its solubility, DME can be dissolved in water and injected into the reservoir through water injection. Upon contacting the fluids in the reservoir, DME immediately partitions into the trapped oil, leading to a reduction in viscosity and swelling of the oil. Due to this partitioning and reduction in viscosity, the mobility of the oil phase increases, making it easier to be displaced leading to an increase in recovery and a reduction in the remaining oil saturation (Chernetsky *et al.*, 2015; Parsons *et al.*, 2016). As the effectiveness of this technology depends on the back production and re-use of DME, a DME-free water chase is carried out to recover the remaining mobile oil and DME (Chernetsky *et al.*, 2015; te Riele *et al.*, 2016). DEW can be implemented from the start in a new water-flood scheme as a secondary recovery method or as part of an ongoing water-flood as a tertiary process without making many changes to the existing infrastructure (Chernetsky *et al.*, 2015; Groot *et al.*, 2016b). Additionally, the DEW method can be applied to different reservoirs and conditions e.g. it works well in low and high permeability reservoirs and can be applied in sandstone and carbonates (Groot *et al.*, 2016b).

The performance of the DEW method is highly dependent on the phase behaviour of the system (Groot *et al.*, 2016a). Several factors such as the partition coefficient (K-value), pressure, temperature, compositional characteristics of the oil, DME concentration in oil as well as the salinity of the aqueous phase affect the swelling and property changes of the oil (Ratnakar *et al.*, 2016c). Therefore, to fully understand the DEW process, the effects of these factors need to be well understood.

3.1 Description of the DEW Concept

Figure 11 conceptually shows how the DEW process works at reservoir and pore scale. As can be observed from the figure, there is still a remaining oil saturation in the reservoir after primary depletion in step 1 and water-flooding in step 2. In step 3, the DME/water mixture is injected into the reservoir. As the mixture contacts the oil, DME partitions into the trapped oil depicted in step 4. This immediately leads to the swelling of the oil phase as well as a reduction in its viscosity. In step 5, the swelling effect increases the saturation of the oil phase making it more mobile and forming an oil bank, which is then displaced by the water-flooding. At the end of the process, a residual saturation of oil and DME still remains trapped in the reservoir as depicted in step 6. This remaining DME can be partially recovered since it is soluble in water. Therefore, in the final step, a chase water flood is carried out and the DME is recovered from the produced water stream at the surface and reused in other areas of the field. The bottom graph plots the recovery factor (RF) against time and shows an increase in RF after the injection of the DME/water mixture.

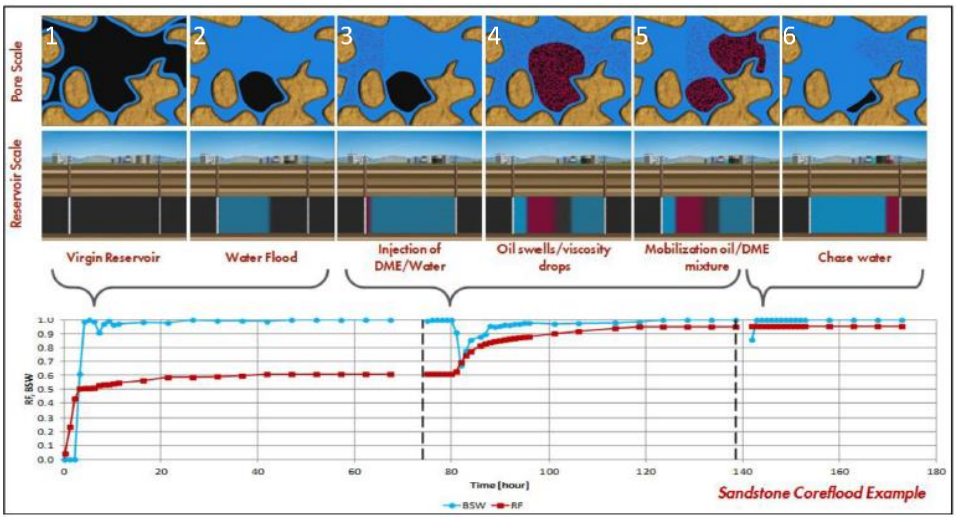

Figure 11 - Simplified Visualization of the DME Process with Phases of Activities Mapped Against the Experimental Results of Sandstone Core flood Undergoing the same Sequence of Flooding Events (Parsons et al., 2016)

Due to the high cost of using DME, the reuse of the solvent is of paramount importance. It is technically possible to fully recover the injected DME from the formation with proper reservoir management. However, losses due to dispersion or losses to fractures and aquifers are inevitable (te Riele *et al.*, 2016). Based on a detailed field development plan carried out by (te Riele *et al.*, 2016), up to 90% of DME can be recovered and reinjected in nearby flood patterns. Therefore, maximising the amount of DME recovered would generally lead to a high net utilization of the solvent making the unit technical cost in DEW competitive with other well established EOR processes (Chernetsky *et al.*, 2015; Parsons *et al.*, 2016; te Riele *et al.*, 2016).

3.2 Salinity

One of the factors that affect the level of DME partitioning in the oil phase is the salinity of the aqueous solution. It controls how much of DME moves from the aqueous to the oil phase (Ratnakar *et al.*, 2016b). Salt only affects the solubility of DME in water, leading to a reduced concentration for the same activity. The activity in the oleic phase remains the same as the concentration in the oleic phase. A fundamental research of the effect of salinity on the solubility of DME in the aqueous phase was carried out by (Chernetsky *et al.*, 2015). Using light Middle Eastern crude (34 API) and NaCl as the salt at the temperature of 50^{o} C - the results shown in Figure 12 were obtained. As can be observed, the solubility of DME decreases as the concentration of the salt increases with a weaker dependence on pressure (Chernetsky *et al.*, 2015). Another experiment carried out by (Ratnakar *et al.*, 2016a) in an attempt to model the DME-brine-crude system shows that increase in temperature decreases the solubility of DME in the aqueous phase (see Figure 13).

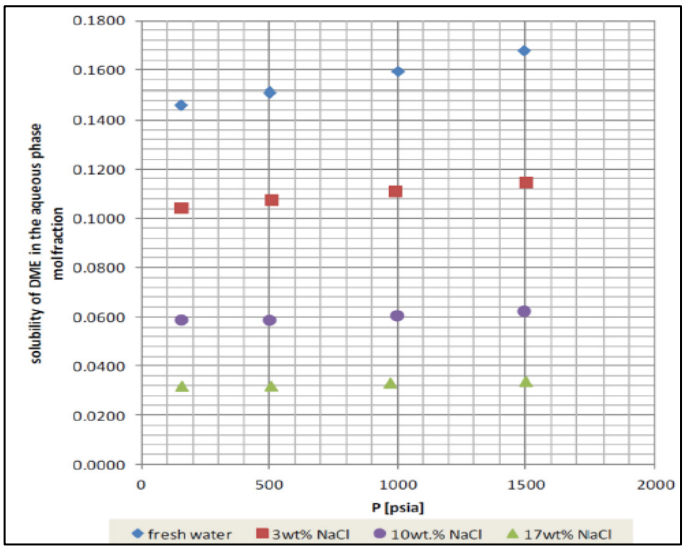

Figure 12 - Solubility of DME in NaCl Brines at 50°C (Chernetsky et al., 2015)

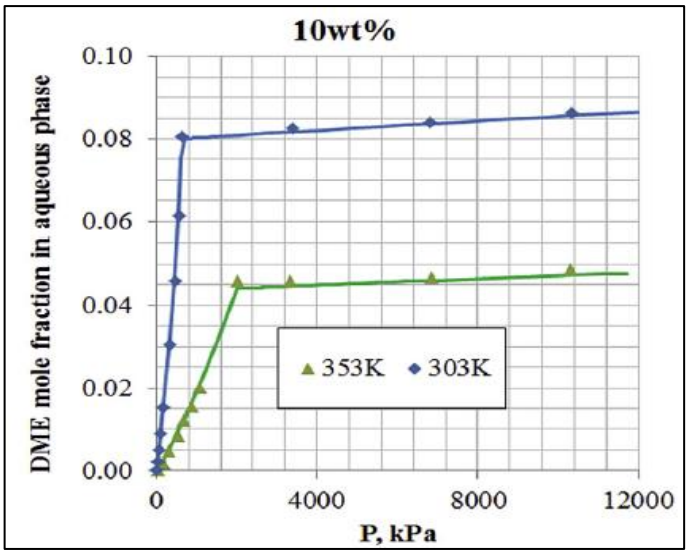

Figure 13 - Solubility of DME in Water at Different Temperatures (Ratnakar et al., 2016a)

Additionally, experiments carried out by (Ratnakar *et al.*, 2016b) showed the dependency of the partitioning coefficient on the salinity of water. The results measured at reservoir condition showed that the K-value (ratio of the mole fraction of DME in the oleic phase to the mole fraction of DME in the aqueous phase) of DME is strongly dependent on the salt concentration of brine at a given temperature and pressure. This is shown in Figure 14.

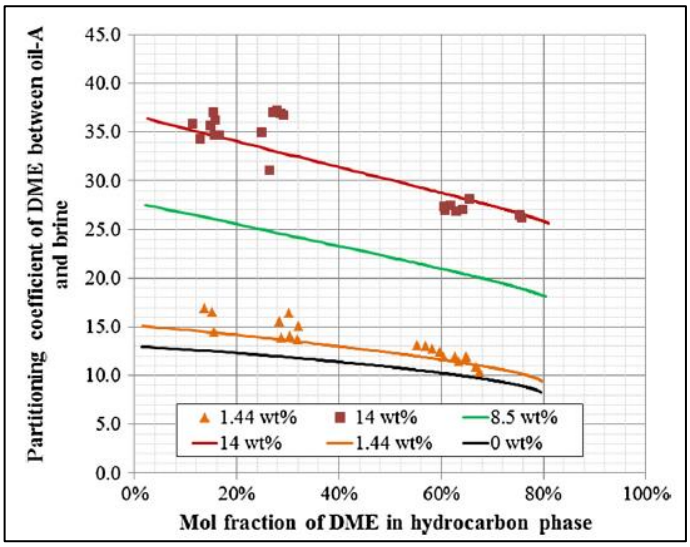

Figure 14 - DME Partitioning between Oil and Brine (of varying salinity) at Reservoir Conditions: 343 K and 17,236 kPa: Marker Points Corresponds to Experiments and Solid Line Corresponds to CPA Model (Ratnakar et al., 2016b)

Generally, the efficiency of high salinity DEW is lower than that of low salinity DEW (Groot *et al.*, 2016b). This can be explained from the fact that the solubility of DME in water decreases as the salinity increases. This is because as the solubility decreases, less DME can be injected during the DEW process (Groot *et al.*, 2016b). However, this also leads to a higher K-value because as the mole fraction of DME in the aqueous phase decreases, the K-value increases. This inverse relationship (see Figure 15) between K-values and wt.% of DME means that, for a low DME concentration, more PV of brine has to be injected in order to attain similar recovery factor as in the case of low salinity (Groot *et al.*, 2016b).

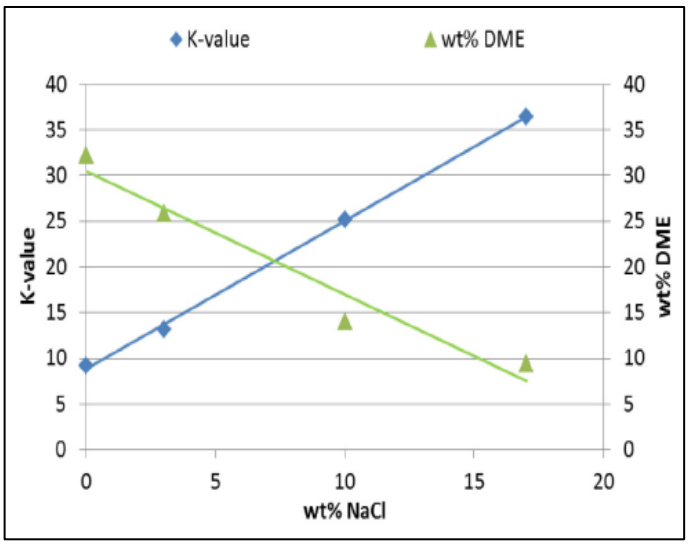

Figure 15 - DME Solubility and K-values vs Salinity (50^0C and 100 bar) (Groot et al., 2016b)

3.3 Field Development Concept

In order to have an optimal DEW process, additional surface facilities are needed. These include DME-water-flood facilities, options for DME supply or production onsite, and surface facilities for the recovery of the back produced DME (Parsons *et al.*, 2016; te Riele *et al.*, 2016). Recently, te Riele *et al.* (2016) came up with a detailed concept for the DEW process. This is schematically shown Figure 16.

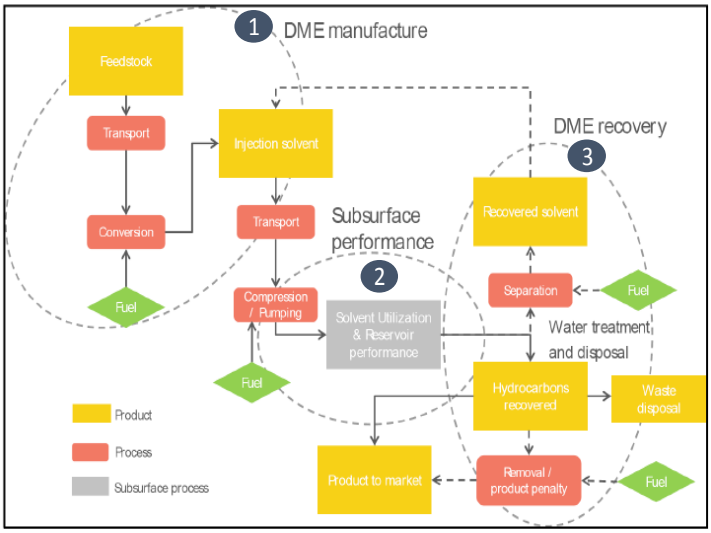

Figure 16 - Schematic Development Lay-out for DEW Process (te Riele et al., 2016)

Figure 16 shows three different stages in the process. Stage 1 involves the manufacturing (locally needing feedstock for the process) and/or supply of DME to the field. Once in the field, DME can be injected into the reservoir. Stage 2 involves the subsurface recovery of oil and solvent. As the success of DEW relies on the back production of DME, it is paramount that the maximum amount of recoverable DME (losses to aquifer, fractures or due to dispersion cannot be avoided) is recovered from the subsurface - proper reservoir management is necessary for this goal to be achieved. Furthermore, a dense well spacing with short pore volume injection times is needed to reduce the residence time (duration between solvent injection and oil recovery) of the solvent in the subsurface. In stage 3, the produced fluid is treated and the solvent is recovered for reinjection in existing or new flood patterns (te Riele *et al.*, 2016). The timing and duration of a single pattern DME recovery determines how much DME is available for reinjection at any given time (te Riele *et al.*, 2016). See te Riele *et al.* (2016) for a detailed field development plan of the DEW process.

3.4 DEW Modelling (Simulation)

A simple one-dimensional (1-D) two-phase system is used to study the mechanism of the DEW process. For simplicity, gravitational forces are disregarded. Figure 17 shows a sketch of the domain with an injector on the left and a producer on the right. In order to understand the process, a numerical model is developed and the equations are solved using the commercial finite element package (COMSOL Multiphysics).

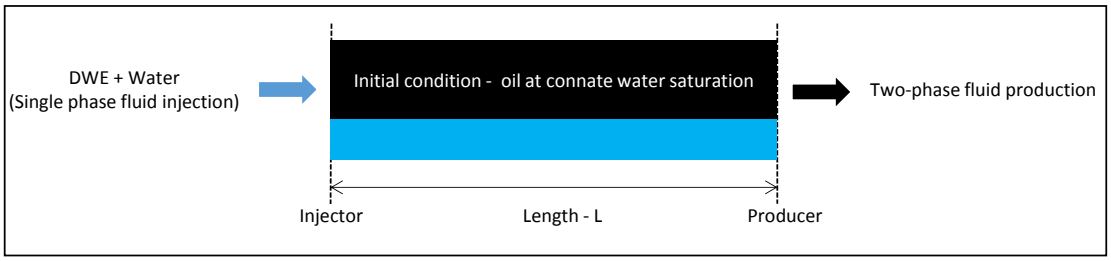

Figure 17 - One-Dimensional Representation (Adapted from (Groot et al., 2016b))

To accomplish this, mass conversation equations for each of the components – oil (e.g. hexadecane), brine and DME are written. Eqs. (24), (25) and (26) give the mass conservation equation for water, oil and DME respectively (Blom *et al.*, 2016; Chahardowli and Bruining, 2014).

$$\varphi\partial_t(S_w\rho_a x_{wa}) + \partial_x u\rho_a x_{wa} f_w - \partial_x\left(D_{cap}\rho_a x_{wa}\partial_x S_w\right) - \partial_x\left(S_w D_m \partial_x(\rho_a x_{wa})\right) + \varphi\partial_t(S_o\rho_o x_{wo}) + \partial_x u\rho_o x_{wo} f_o + \partial_x\left(D_{cap}\rho_o x_{wo}\partial_x S_w\right) - \partial_x\left(S_o D_m \partial_x(\rho_o x_{wo})\right) = 0, \quad (24)$$

$$\varphi\partial_t(S_w\rho_a x_{oa}) + \partial_x u\rho_a x_{oa} f_w - \partial_x\left(D_{cap}\rho_a x_{oa}\partial_x S_w\right) - \partial_x\left(S_w D_m \partial_x(\rho_a x_{oa})\right) + \varphi\partial_t(S_o\rho_o x_{oo}) + \partial_x u\rho_o x_{oo} f_o + \partial_x\left(D_{cap}\rho_o x_{oo}\partial_x S_w\right) - \partial_x\left(S_o D_m \partial_x(\rho_o x_{oo})\right) = 0, \quad (25)$$

$$\varphi\partial_t(S_w\rho_a x_{da}) + \partial_x u\rho_a x_{da} f_w - \partial_x\left(D_{cap}\rho_a x_{da}\partial_x S_w\right) - \partial_x\left(S_w D_m \partial_x(\rho_a x_{da})\right) + \varphi\partial_t(S_o\rho_o x_{do}) + \partial_x u\rho_o x_{do} f_o + \partial_x\left(D_{cap}\rho_o x_{do}\partial_x S_w\right) - \partial_x\left(S_o D_m \partial_x(\rho_o x_{do})\right) = 0, \quad (26)$$

where φ is the porosity, $x_{w\alpha}$, $x_{o\alpha}$ and $x_{d\alpha}$ are the mole fractions of water, oil and DME in phase α respectively (α = a (aqueous phase), o (oleic phase), ρ_o and ρ_a are the molar densities of the oleic and aqueous phase and thus $\rho * x$ in the equations above gives the molar concentration, u is the Darcy velocity, f_w is the fractional flow of water, S_o is the oil saturation, S_w is the water saturation and D_{cap} and D_m are the capillary and molecular diffusion, respectively. For simplicity, both D_m and D_{cap} are assumed to be equal and constant. COMSOL uses a central differencing method. Therefore, diffusion has to be explicitly included for stability.

Because the sum of the mole fractions in either the aqueous or oleic phase sums up to one, the equations are added to get a total equation (see Eq. (27)).

$$\partial_t(S_w\rho_a) + \partial_x u\rho_a f_w - \partial_x\left(D_{cap}\rho_a\partial_x S_w\right) - \partial_x(S_w D_m\partial_x\rho_a) + \varphi\partial_t(S_o\rho_o) + \partial_x u\rho_o f_o + \partial_x\left(D_{cap}\rho_o\partial_x S_w\right) - \partial_x(S_o D_m\partial_x\rho_o) = 0. \quad (27)$$

Based on the Darcy equation for multiphase flow, we obtain for the fractional flow function f_w (see Eq. (28)).

$$f_w = \frac{\frac{k_{rw}}{\mu_a}}{\frac{k_{rw}}{\mu_a}+\frac{k_{ro}}{\mu_o}}, \quad (28)$$

where k_{rw} is the relative permeability of water, k_{ro} is the relative permeability of oil, μ_a is the viscosity of the aqueous phase and μ_o is the viscosity of the oleic phase. The phase viscosity is used in this case in place of the component viscosity. Viscosity reduction is one of the mechanisms that contribute to the recovery of oil using DME. The viscosities are obtained using a quarter-power law shown in Eqs. (29) and (30) (Chahardowli and Bruining, 2014), i.e.:

$$\mu_a = \left(\frac{\frac{x_{da}*Vol_{a-dme}}{\mu_{dme}{}^{1/4}} + \frac{x_{wa}*Vol_w}{\mu_w{}^{1/4}}}{x_{da}*Vol_{a-dme} + x_{wa}*Vol_w}\right)^{-4}, \quad (29)$$

$$\mu_o = \left(\frac{\frac{x_{do}*Vol_{o-dme}}{\mu_{dme}{}^{-1/4}} + \frac{x_{oo}*Vol_{dec}}{\mu_{dec}{}^{-1/4}}}{x_{do}*Vol_{o-dme} + x_{oo}*Vol_{dec}}\right)^{-4}, \quad (30)$$

where Vol_{a-dme} is the volume of DME in aqueous phase, Vol_{o-dme} is the volume of DME in the oleic phase, Vol_w is the molar volume of water, Vol_{hex} the partial molar volume of hexadecane, μ_{dme} viscosity of pure DME, μ_w the viscosity of water and μ_{hex} is the viscosity of hexadecane.

The relative permeability curves are obtained by using the Brooks-Corey correlation as shown in Eqs. (31) and (32) below:

$$k_{rw} = k_{rw}{}^{e}\left(\frac{S_w - S_{wc}}{1 - S_{wc} - S_{or}}\right)^{n_w}, \quad (31)$$

$$k_{ro} = k_{ro}{}^{e}\left(\frac{1-(S_w - S_{wc})}{1 - S_{wc} - S_{or}}\right)^{n_o}, \quad (32)$$

where $k_{rw}{}^{e}$ is the end point permeability of water and $k_{ro}{}^{e}$ is the end point permeability of oil. n_w and n_o are the saturation exponent for water and oil respectively.

The molar densities of the phases are calculated using the volume concentration of the phases as shown in Eqs. (33) and (34) (Chahardowli and Bruining, 2014), i.e.:

$$\rho_o = \frac{1}{\frac{x_{oo}}{\rho_{hex}} + x_{do}*Vol_{o-dme}}, \quad (33)$$

$$\rho_a = \frac{1}{\frac{x_{wa}}{\rho_w} + x_{da} * Vol_{a-dme}}, \tag{34}$$

where ρ_{hex} and ρ_w are the densities of the pure components, hexadecane, and water respectively.

Boundary conditions are needed to solve these equations. For the water equation in Eq. (24), the boundary and initial conditions are given in Eqs. (35), (36) and (37), i.e.:

$$S_w(x = 0, t) = 1 - S_{or}, \tag{35}$$

$$S_w(0, t = 0) = S_{wc}, \tag{36}$$

$$\partial_x S_w(x = L) = 0, \tag{37}$$

where S_{or} is the residual oil and S_{wc} denotes the connate water. L is the length of the reservoir.

The boundary and initial conditions of the DME equation (see Eq. (26)) are given in Eqs. (38), (39) and (40), i.e.:

$$x_w(x = 0, t) = x_{wo}, \tag{38}$$

$$x_w(0, t = 0) = 0, \tag{39}$$

$$\partial_x x_w(x = L) = 0. \tag{40}$$

3.4.1 Phase Behaviour using the UNIFAC Method

The DEW method is a phase-driven process. Therefore, in order to successfully model the process, a suitable phase diagram is needed. For this thesis since only a limited number of experimental data are available in the literature; a semi-empirical method is used to get an idea of the liquid-liquid equilibrium (LLE) of the mixture. UNIFAC (UNIQUAC Functional-groups Activity Coefficients), the method used in this case calculates the activity coefficients (account for deviation from ideal situation) by using the functional groups of the molecules present in the liquid mixture (Muzenda, 2013). For example, the functional groups in DME are CH_3O and CH_3, in hexadecane - CH_3 and CH_2, and H_2O as the only functional group for water. Details of the UNIFAC method can be found in (Hooper *et al.*, 1988; Muzenda, 2013). The accuracy of the UNIFAC method depends largely on how optimized the interaction parameters are for the specific mixture. Owing to the generality of the model, it tends not to be very accurate for a specific class of mixtures (Hooper *et al.*, 1988). There are also several factors that reduce the accuracy of the method. First, the accuracy is only guaranteed within certain temperature ranges and only suitable for systems at low to moderate pressures (Muzenda, 2013). It is also difficult to model the system close to the critical zone (Muzenda, 2013). Having these limitations in mind, Hooper *et al.* (1988) came up with a modified UNIFAC method just for water-hydrocarbon systems at wide temperature ranges. However, in his modified model, he could only come up with interaction parameters for seven organic groups of which those of interest to us were not included. Therefore, it was not possible to take advantage of the accuracy in the modified method developed by Hooper *et al.* (1988).

The original UNIFAC model was thus used to determine the LLE of the mixture using DWSIM a chemical process simulator (Medeiros, 2008). The results obtained from the simulation are plotted in the ternary diagram in Figure 18 below.

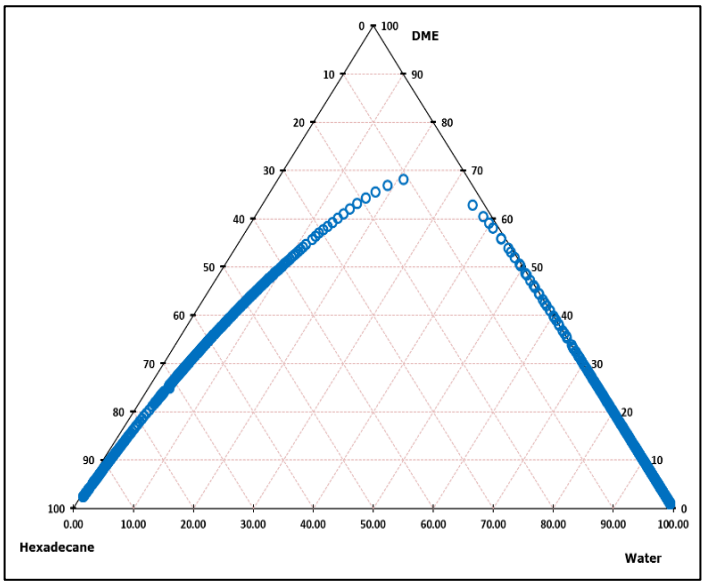

Figure 18 - Ternary Diagram for DME/Hexadecane/Water System

Figure 18 represents the single and two phase regions and shows DME's preference to partition into the oleic phase based on the end points of the tie lines.

Having obtained the phase behaviour, the model equations given in Eqs. (24), (25) and (26) are transformed into weak forms and implemented in COMSOL. COMSOL offers to use the weak formulation, which is closer to the finite element formulation.

3.4.2 Results and Discussions

Table 4 gives the input parameters and variables used for the COMSOL simulation.

Table 4 - Summary of Parameters and Variables

Parameter	**Symbol**	**Value**	**Unit**
Diffusion coefficient	D_M	2.0×10^{-9}	m^2/s
End point oil permeability	k_{roa}	1	[-]
End point oil permeability	k_{rwa}	0.5	[-]
Length of reservoir	L	200	M
Hexadecane (oil) viscosity	μ_o	1.89×10^{-3}	Pa.s
Water viscosity	μ_w	1.0×10^{-3}	Pa.s
Ether viscosity	μ_{dme}	1.5×10^{-3}	Pa.s
Molar weight hexadecane	M_{hex}	0.226	kg/mol
Molar weight DME	M_{dme}	0.0461	kg/mol
Molar weight water	M_{water}	0.018	kg/mol
Water saturation exponent	n_w	2	[-]
Oil saturation exponent	n_o	2	[-]
Peclet number	N_{pe}	25000	[-]
Permeability	K	1.0×10^{-12}	m^2
Porosity	φ	0.3	[-]
Molar density DME	ρ_{dme}	14500	mol/m^3
Molar density water	ρ_{water}	55508	mol/m^3
Molar density hexadecane	ρ_{hex}	3400	mol/m^3
Boundary water saturation	S_{bound}	0.7	[-]
Connate water saturation	S_{wc}	0.2	[-]
Residual oil	S_{or}	0.3	[-]

Parameter	Symbol	Value	Unit
Injection velocity	u_{inj}	1.0×10^{-5}	m/s
Pore volume	PV	60	m
DME injection start time	t_{st}	3.0×10^{6}	s
DME injection end time	t_{end}	9.0×10^{6}	S
Molar volume of water	V_w	1.80×10^{-5}	m^3/mol
Molar volume of DME	V_{dme}	5.83×10^{-4}	m^3/mol
Molar volume of hexadecane	V_{hex}	2.94×10^{-4}	m^3/mol
Mole% of DME	x_{bound}	0.63	[-]

Figure 19 shows the viscosity of the oleic phase. As can be observed, the viscosity of the mixture of DME and hexadecane has a lower viscosity than the viscosity of pure DME, which is expected since this partly contributes to the overall mechanism of the DEW process.

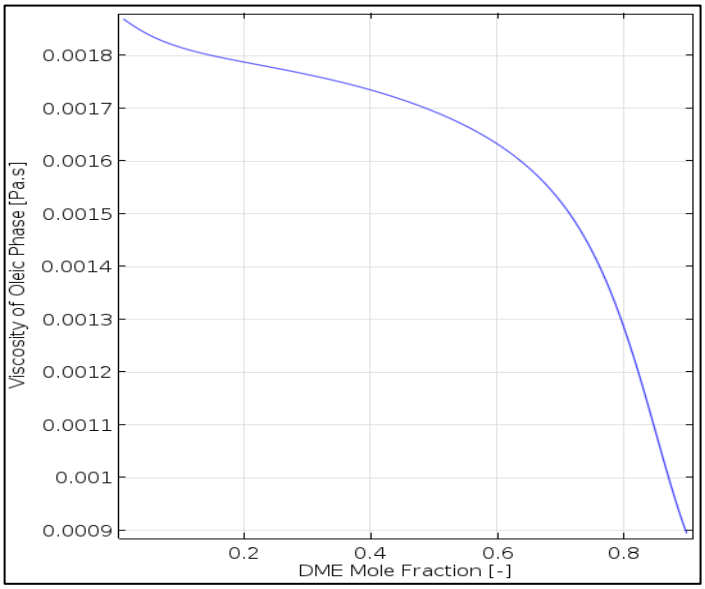

Figure 19 - Viscosity of DME and Hexadecane Mixture using the quarter power law Eqs. (29) and (30)

Next, we discuss a displacement process where we inject first 0.5 PV of fresh water, then a DME slug of 1 PV followed by injection of a fresh water slug of 1.2 PV. This injection scheme is shown in Figure 20.

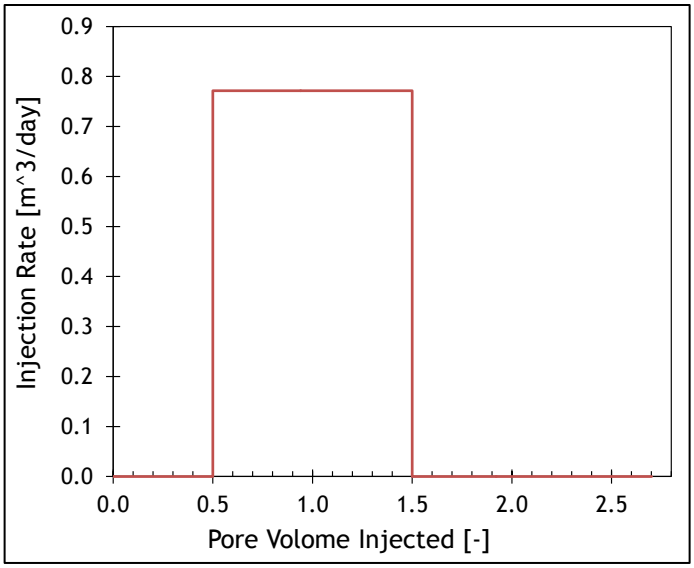

Figure 20 - DME Injection Sequence

Figure 21 shows the ensuing aqueous phase saturation profile during water injection before breakthrough with a maximum water saturation level at 1-S_{or} and minimum at S_{wc}. We omitted the saturation profiles after breakthrough. The oil viscosity is low (light oil) leading to a low mobility ratio and a fractional flow function (see Appendix E), which moves to high saturations. We expect a piston like displacement as is indeed shown. The mesh is 0.01 [m].

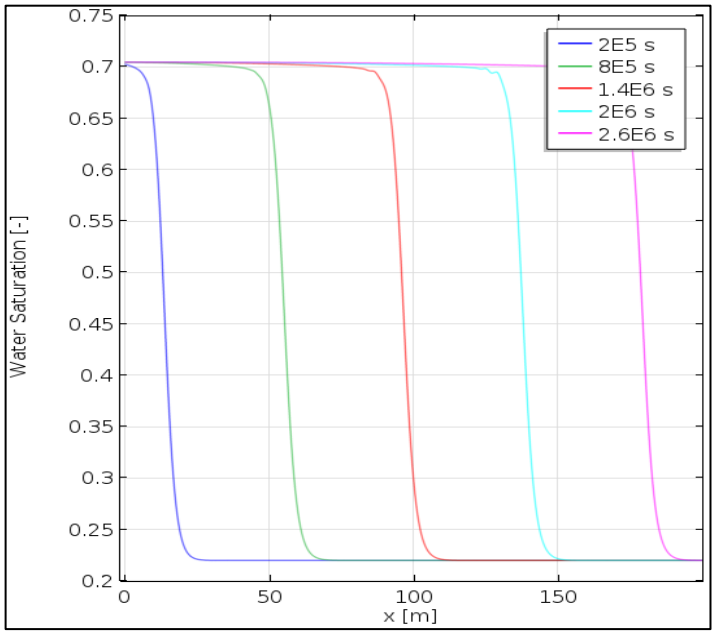

Figure 21 - Water Saturation Profile before DME Injection

Figure 22 shows the K value, i.e. the ratio between the DME concentration in the oleic phase and in the aqueous phase. The figure shows that the K-value is strongly concentration dependent, where the relative amount of DME in the oleic phase is about nine times as large in the oleic phase than in the aqueous phase for mole fractions below 0.1, whereas above 0.6, the DME in the oleic phase is about 1.2 times the DME concentration in the aqueous phase. The velocity of the oleic phase is higher than the velocity in the aqueous phase due to the fact that oil saturation downstream is higher than the water saturation. It is asserted that this also causes the broadening of the DME wave. Moreover, at the boundary, we specify the derivative of the concentration to be zero (see Eq. (40)), which is why the DME concentration towards the boundary becomes horizontal (zero) (see Figure 23).

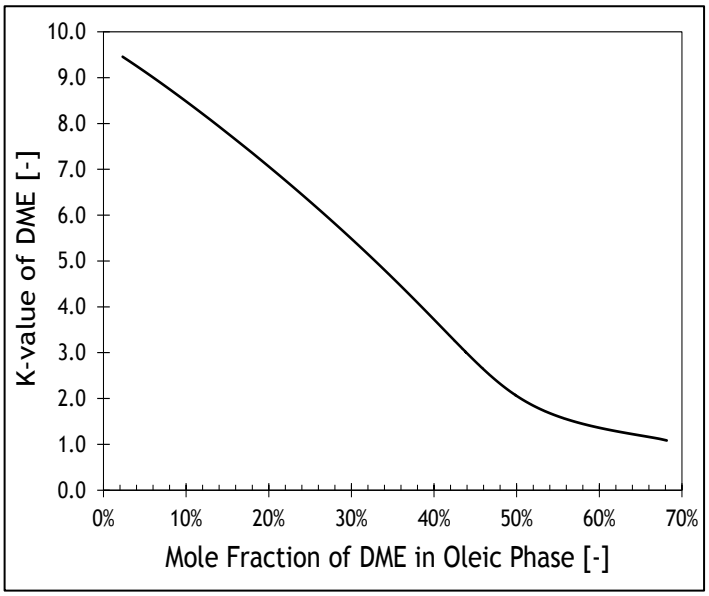

Figure 22 – K-value (mol-frac DME in oleic divided by DME in Aqueous Phase, i.e. DME Partitioning Coefficient between the Aqueous and Oleic Phase

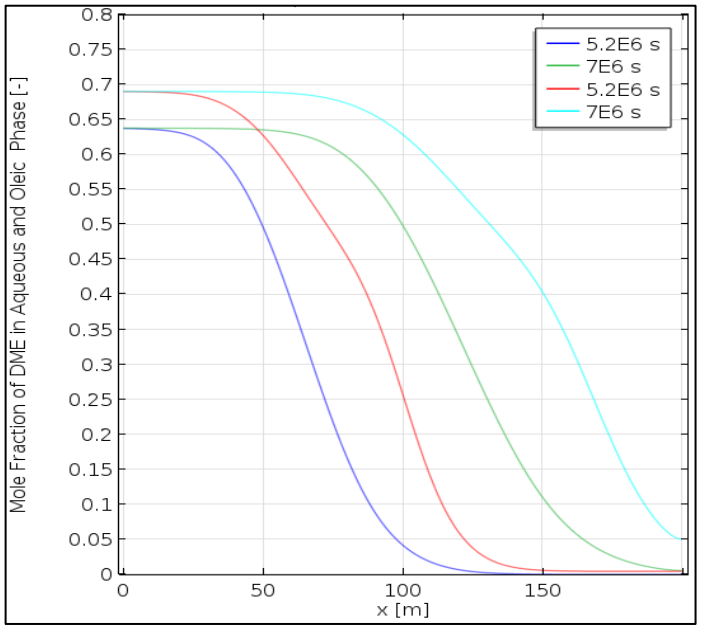

Figure 23 - Mole Fraction of DME in Aqueous Phase (Blue and Green) and Oleic Phase (Red and Cyan)

Figure 24 shows the concentration profile of DME in the aqueous phase after DME injection at 0.5 PV to 1.5 PV. We inject DME in water at a mole fraction of 63%. As can be observed, the concentration profiles start from about 0.63, which is the maximum concentration of DME in the aqueous phase and gradually reduces as it moves from the injector to the producer. This is because as it gets in contact with the oil, it gradually partitions into the oleic phase. This phenomenon is observed when DME is injected i.e. from 3.6 x 10^6 s to 9 x 10^6 s. After this time, the injection of DME is stopped. After the DME slug of 1PV, we apply a chase water flood. As a result, the DME concentration at the injection side starts to decrease, whereas the DME in the system starts to move towards the production well.

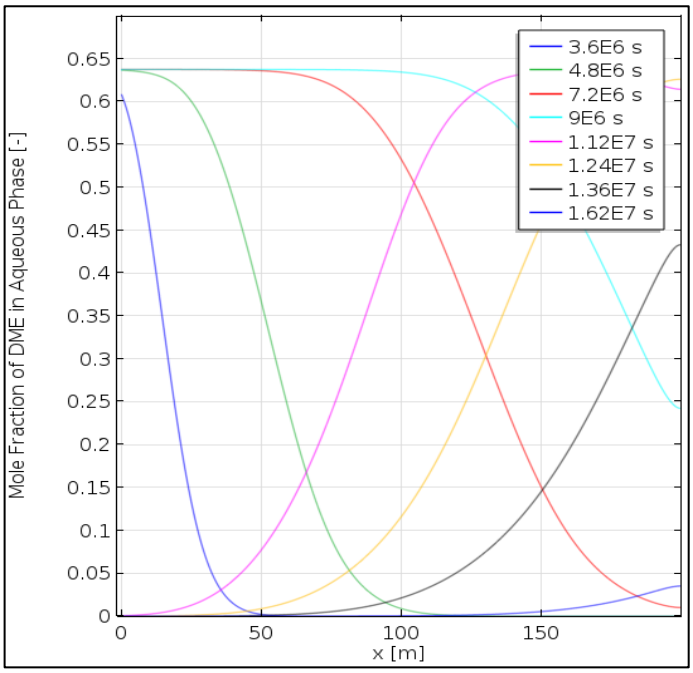

Figure 24 – DME Concentration in the Aqueous Phase

The mole fraction of hexadecane in the oleic phase is shown in Figure 25. Further reduction is observed at time 3.4 x 10^6 s because of the continuous injection on DME leading to a higher cumulative amount of DME in the system. This confirms the fact that DME partitions between the oleic phase and the aqueous phase, when the phases are in contact. As can be observed in the figure, before injecting DME, the oleic phase only contains hexadecane (2.8 x 10^6 s). In the next time step i.e. at 3.2 x 10^6 s, the mole fraction of hexadecane is reduced due to the presence of DME in the oleic phase. Indeed, when after half a PV of pure water injection we start to inject DME and consequently the hexadecane concentration at the injection side decreases. After we reverse to pure water injection, the hexadecane diluted with DME moves towards the production well, leaving a small amount (smaller than the residual oil) of hexadecane. However, the mole fraction of hexadecane reverses back to one towards the end of the simulation i.e. at times 1.58 x 10^6 s and 1.62 x 10^6 s at the injection side where pure water is injected.

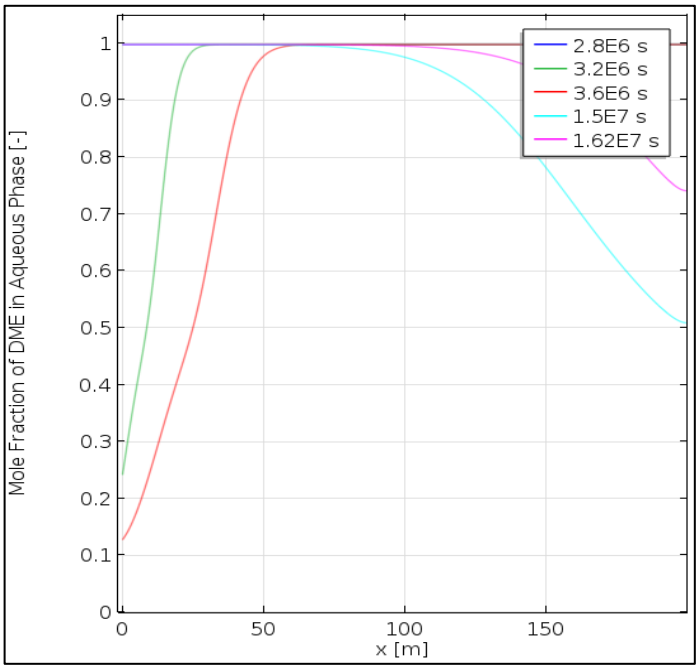

Figure 25 - Mole Fraction of DME in the Oleic Phase

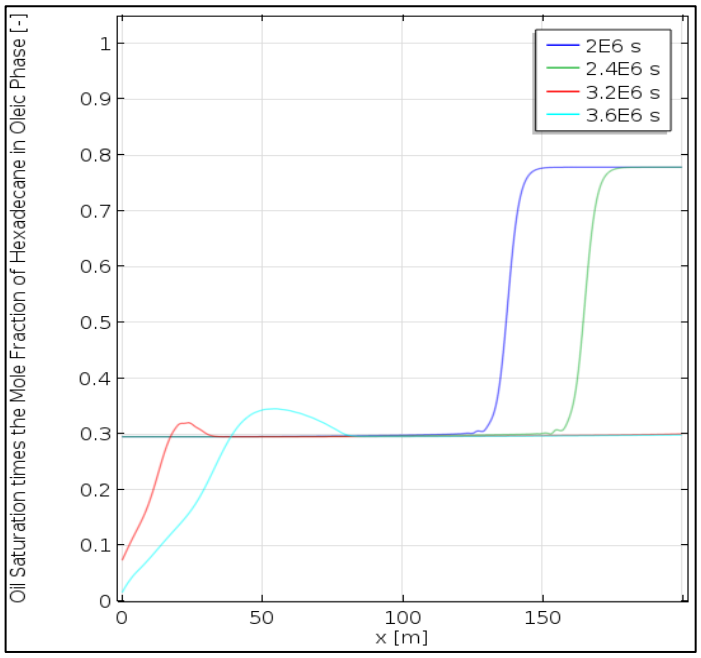

Figure 26 - Oil Saturation times the Mole Fraction of Hexadecane in the Oleic Phase

Figure 26 shows the oil (hexadecane) saturation times the mole fraction of hexadecane in the oleic phase before and during DME injection. At times 2 x 10^6 s and 2.4 x 10^6 s, the oil saturation shows a typical Buckley-Leverett saturation profile before breakthrough (before DME injection). At times 3.2 x 10^6 s and 3.4 x 10^6 s (DME injection), an oil bank is formed depositing hexadecane from upstream towards the downstream part.

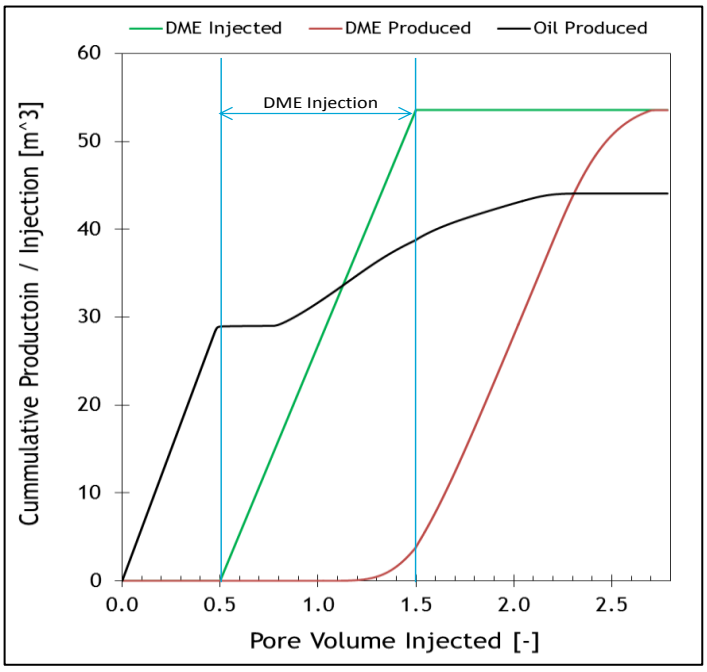

Figure 27 - Cumulative Injection and Production

We use a 1-D simulation to determine the cumulative injection of DME and cumulative production of DME and oil. This is shown in Figure 27 and Figure 28, where we divide by the OIIP (oil initially in place). Figure 28 shows that about 92% of the oil in place is recovered using DME. This includes about 30% incremental production after water flooding. The overall recovery factor obtained is similar to that obtained by (Chernetsky *et al.*, 2015). 100% of the DME injected is recovered.

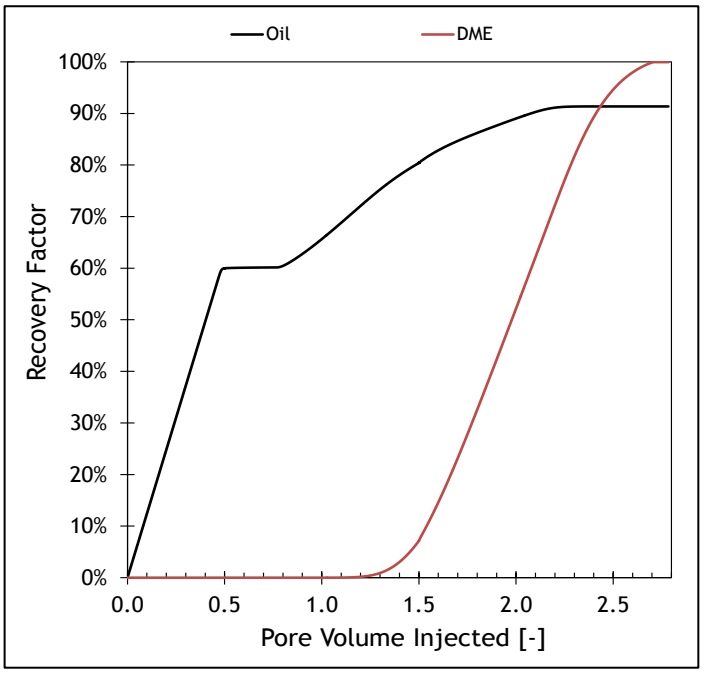

Figure 28 - Recovery Factors of Oil and DME

3.4.2.1 Sensitivity Analysis

For the sensitivity analysis, three main variables are considered. First, the mesh size, secondly, the Peclet number and finally, the DME concentration in the aqueous solution.

Mesh Size

Three cases are considered. Grid cells with mesh sizes 10 m, 1 m and 0.1 m. All other parameters are kept constant as in Table 4. The effect of the mesh size is shown on the DME concentration in the aqueous in Figure 29 and the saturation profile in Appendix F. The mesh size of 10 m (A) leads to numerical errors. Increasing the mesh size to 1 m (B) and consequently to 0.1 m (C) increases the accuracy of the simulation with no significant difference between 1 m and 0.1 m.

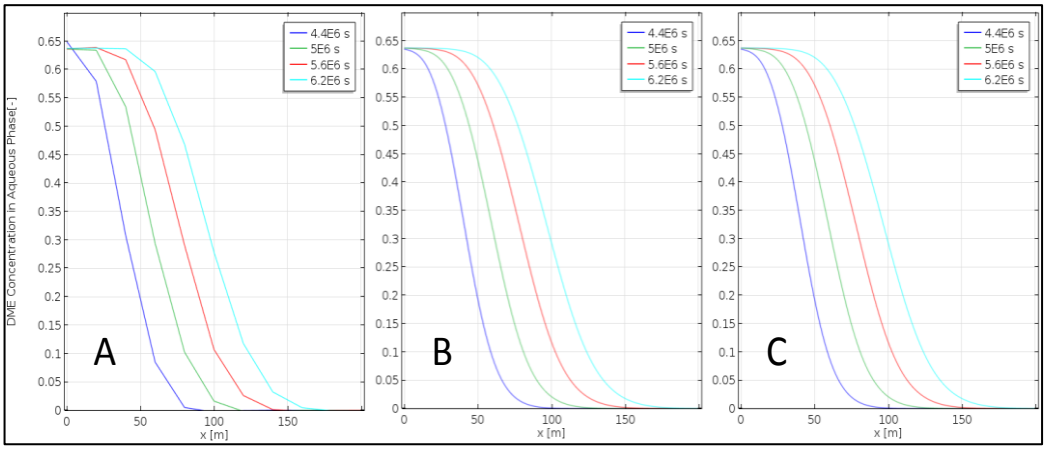

Figure 29 – DME Concentration in the Aqueous Phase for Mesh Size 10 m (A), 1 m (B) and 0.1 m (C)

Peclet Number

Diffusion is explicitly included in the model for the purpose of stability since COMSOL uses the central differencing method, which does not take this into account. This is represented in the model using the Peclet number (N_{pe}). N_{pe} is the ratio of advection (or convection) to dispersion, the two transport phenomenon involved (Peters, 2012). In order to determine the sensitivity of N_{pe} on the results of the model, three different scenarios are considered: N_{pe} of 5000 (A), 10000

(B) and 25000 (C). A mesh size of 0.1 m is used - leaving all other parameters in Table 4 constant.

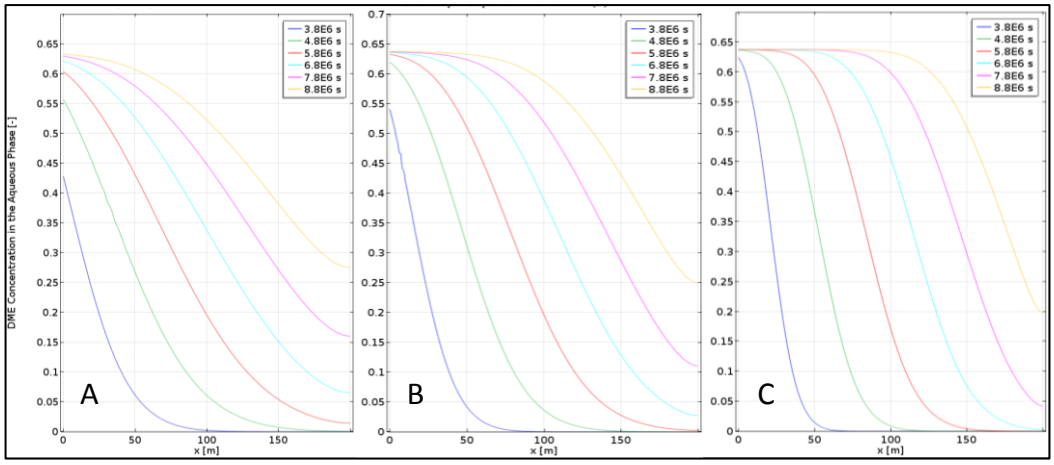

Figure 30 - DME Concentration Profile in the Aqueous Phase [A - N_{pe} of 5000; A - N_{pe} of 10000; A - N_{pe} of 25000]

Figure 30 shows the concentration profiles of DME in the aqueous phase with different N_{pe}. As can be observed from the figure, the profiles of A spreads out more with a higher mixing zone length than that of B and C. This is because the diffusion is the highest in A. This has an effect on the overall oil recovery, with C having the highest recovery factor due to a higher advection to dispersion ratio (see Figure 31).

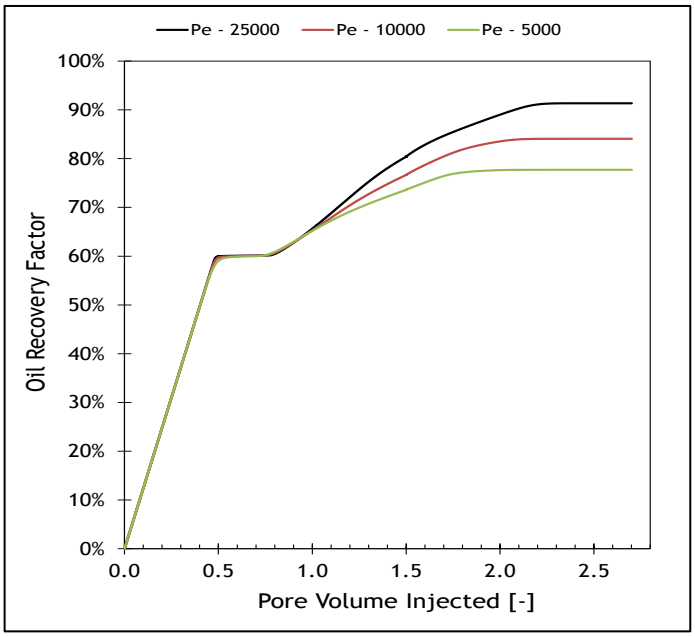

Figure 31 - Oil Recovery Factor for Different Peclet Numbers [A - N_{pe} = 5000; B - N_{pe} = 10000; C - N_{pe} = 25000]

DME Concentration

Four different DME concentrations are used to simulate the effect of increasing the DME concentration in the aqueous solution. The following four cases are considered: 7%, 13%, 30% and 63% in the aqueous phase. A mesh size of 0.1 m is used leaving all other parameters given in Table 4 constant. The oil recovery as well as the incremental oil recovery increases with increasing DME concentration. Figure 32 shows the oil recovery factor for the four different cases. As can be observed, the oil recovery factor increases with increasing DME concentration.

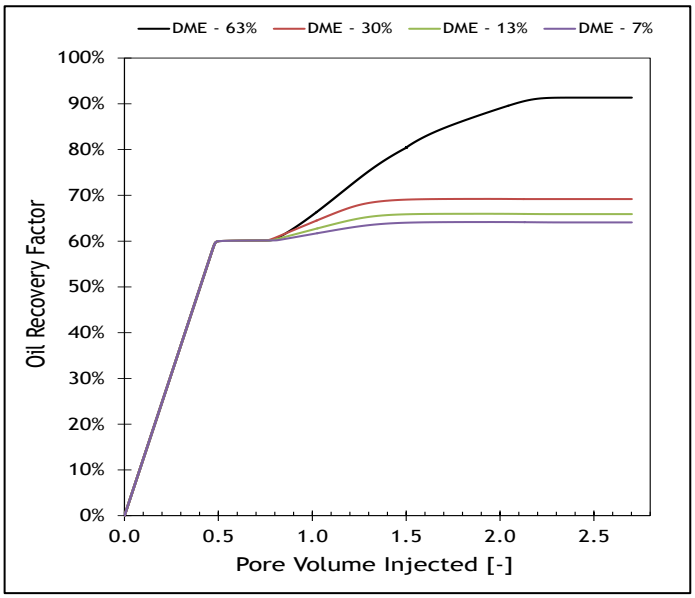

Figure 32 - Oil Recovery Factor at Different DME Concentrations

The simulation gives a good indication of the DEW process and is in line with what can be expected when using DME for EOR. However, there are several factors that limit the accuracy of this work (Hon, 1989). First, the process is highly phase driven, therefore, any erroneous description of the phase behaviour would have a great impact on the simulation results, which is the case here when using UNIFAC based activity coefficients. The phase behaviour is obtained using a semi-empirical UNIFAC method, which is not very accurate. This is why, in order to achieve the same recovery for a simple 1-D model similar to that in (Chernetsky *et al.*, 2015), a concentration of 63 mol% of DME in fresh water is used. This is about five times more than the experimental solubility of DME of ~13% in fresh water reported by Chernetsky *et al.* (2015). For the UNIFAC based phase behaviour, the COMSOL simulation predicts that 100% of the DME injected is produced; however, in practice, only about 90% of the DME injected can be back produced based on any optimised system (te Riele *et al.*, 2016). Recovering 100% of the DME injected in this model can be attributed to the simplicity of the model, which does not consider reduced displacement efficiency and incomplete volumetric sweep.

4 Exergy Analysis of DME-enhanced Waterflooding Process

Exergy in the broad sense is the energy available to do work. Unlike mass and energy, exergy cannot be conserved but rather is consumed to do work (Ptasinski, 2013). This is because it combines both the first and second law of thermodynamics and thus can be used to account for both the quantity and quality of energy and material flows – the quality of energy and materials in any process decreases progressively (Oliveira Júnior, 2013; Ptasinski, 2013). Therefore, the exergy of a system is defined as the highest useful work obtainable from an energy stream when it is brought into equilibrium with its reference environment (Ptasinski, 2013).

Since exergy is an extensive property, just like mass and energy, exergy balances of a system can be written when doing an exergy analysis (Ptasinski, 2013). This balance helps to point out the inefficiencies in the system in form of exergy losses and shows where improvement is necessary. Figure 33 shows a typical exergy balance of a steady flow stream with exergy losses due to irreversibilities (Ptasinski, 2013).

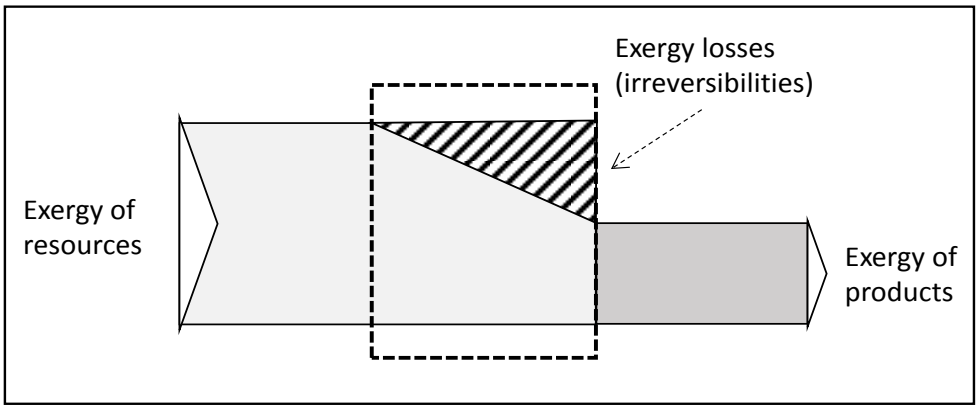

Figure 33 - Exergy Balance (Ptasinski, 2013)

In our case, exergy is made up of four components: potential, kinetic, physical and chemical exergy. The potential and kinetic exergy and energy of a material stream are equal and in most cases are assumed to be negligible when compared with chemical and physical exergy (Farajzadeh *et al.*, 2017; Voldsund, 2014). The physical exergy comprises any effect except for chemical reactions, potential and kinetic energy and accounts for example for the dependence on the aggregate state, pressure and temperature with respect to the aggregate state, pressure and temperature of the dead state. Dead state refers to a state when the system and the environment of choice are in complete thermodynamic equilibrium (Querol *et al.*, 2013; Szargut *et al.*, 1988). The chemical exergy relates to the deviation in chemical composition when compared to the reference substance present in the environment (Tuong-Van Nguyen *et al.*, 2012).

Obtaining the exergy efficiency is one of the goals when doing an exergy analysis. In this case, the exergy efficiency is referred to as the Exergy Recovery Factor (Ex_{RF}) given by Eq. (41) (Eftekhari *et al.*, 2017), i.e.:

$$Ex_{RF} = \frac{Ex_{Resource} - Ex_{invested}}{Ex_{Resource}}. \quad (41)$$

4.1 Exergy and Production Cycle

It is important to come up with an exergy analysis structure before doing any exergy analysis. This structure helps to first identify the main components in the system that would need to be analysed. Thereafter, the system boundary is set. Setting the boundary helps to confine the analysis to those areas of importance to the study. Once the boundary is set, the material and work streams are looked into to determine how much exergy is gained and lost in the process. This gives crucial information on the various components that are most energy intensive in the process. Having identified the most energy intensive components, the focus is then placed on coming up with ways to optimize those processes, which leads to an optimized design that meets both energy and climate challenges. Figure 34 shows the overall exergy analysis structure.

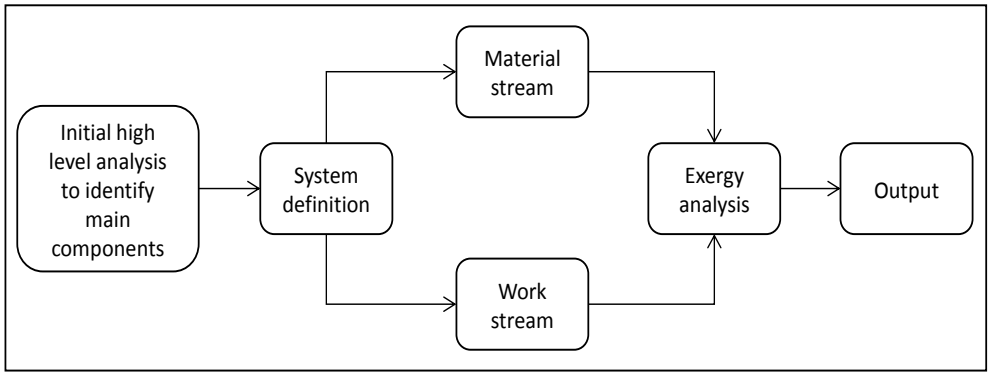

Figure 34 - Exergy Analysis Structure (Farajzadeh et al., 2017)

4.1.1 System Definition

The system is shown as a collection of boxes, also called the nodes. The main nodes looked into in this case include the manufacturing of DME, water treatment, pumping requirements, artificial lifts in the producers, separation and transport to the refinery. The nodes in orange are the exergy consuming processes (exergy invested), while those in green give the exergy gained in the system. The thus produced DME is reinjected or used for other uses. The DME free gas can be utilized as product gas or as feed stock for DME production. Setting a system boundary is important when doing an exergy analysis. Indeed, as can be seen in Figure 35, the boundary is set to only include the upstream part of the DME Enhanced Water-flooding (DEW) method i.e. until when the crude is delivered to the refinery.

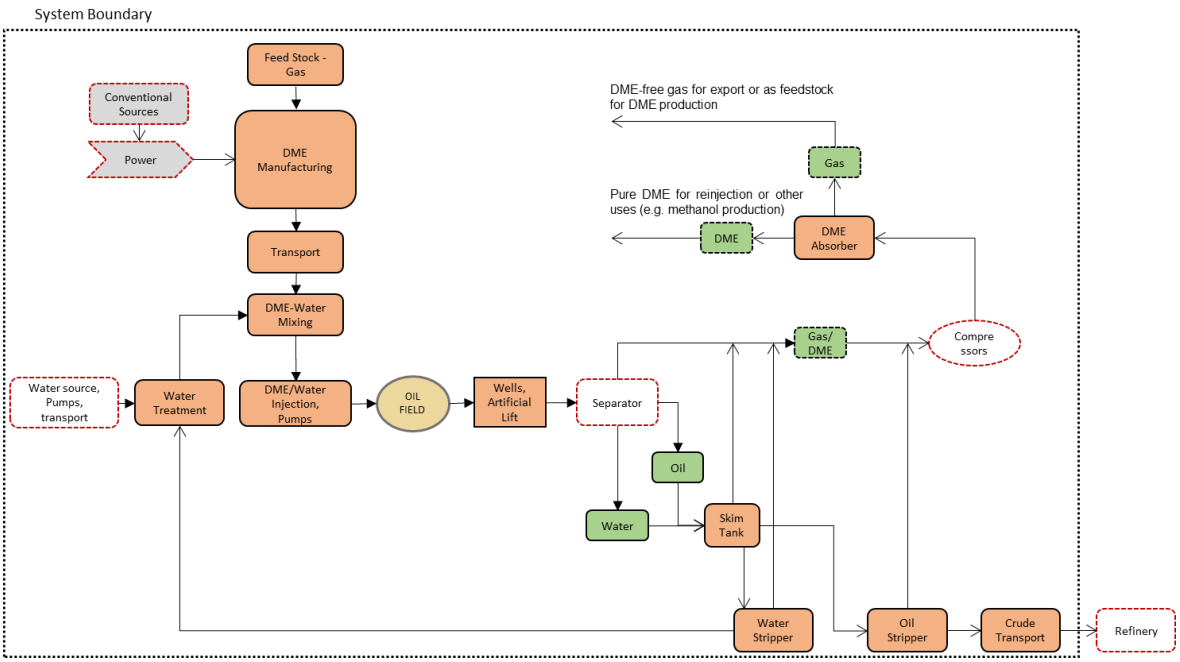

Figure 35 - System Boundary for DEW Process

4.1.2 Material Stream

In this case, the produced hydrocarbon, water and DME are the main material streams. To calculate the exergy of the produced hydrocarbon – oil or gas, the lower heating value is considered (Finnveden and Östlund, 1997; Liu and Li, 2015; Rivero *et al.*, 1999). The lower heating value disregards the condensation of water. The exergy of the products are to be compared to the exergy of the so-called dead state a reference state in the immediate vicinity of where the process is carried out, from which no further exergy can be extracted (Szargut *et al.*, 1988). For convenience, the environment is assumed to be at standard conditions i.e. at temperature of 298.15°K and pressure of 1 bar (101.325 kPa) (Querol *et al.*, 2013; Szargut *et al.*, 1988). The chemical reference exergy is the exergy of the materials such as they occur in the environment (Szargut *et al.*, 1988). However, in practice the reference exergy of the materials is the exergy also in its standard normal form, i.e. at one atmosphere pressure and 298.15 K. Following this, the chemical exergy can be calculated.

Generally, the standard chemical exergy of any component can be calculated from the standard chemical exergy of its elements, which are normally given – see Eq. (42) (Oliveira Júnior, 2013), i.e.:

$$Ex^{ch} = -\Delta G_0 - \left[\sum_i x_i Ex_i^{ch}\right] coreactants + \left[\sum_j x_j Ex_j^{ch}\right] products, \quad (42)$$

where ΔG_0 is the standard Gibbs energies of formation, and x represents the number of moles of the co-reactants and products.

For methane, a typical combustion reaction of methane and oxygen as shown in Eq. (43) is assumed (Oliveira Júnior, 2013), i.e.:

$$CH_4 + 2O_2 \rightarrow CO_2 + 2H_2O\ (g). \quad (43)$$

The standard chemical exergy of methane can be calculated using the reaction of the combustion reaction (Eq. (43)) in Eq. (42), while ignoring condensation of water. The standard exergy of the co-reactant (O_2) and products (CO_2 and H_2) shown in Eq. (43) can be obtained from (Oliveira Júnior, 2013; Sankaranarayanan *et al.*, 2010) and the standard Gibbs of energy of formation of methane is listed in (Smith *et al.*, 2001). This leads to a standard chemical exergy of

methane of 831.65 kJ/mol or 51,978.13 kJ/kg (assuming a molar mass of methane to be 16.04 g/mol). The overall exergy of components are different at different temperatures and pressures. Table 5 shows the exergy value of methane at different pressures and temperatures.

Table 5 - Exergy Values (Methane in kJ/mole) (Sankaranarayanan et al., 2010)

P (bar)	T (^oC)	Exergy (physical)	Exergy (chemical)	Exergy (total)
1	25	0.0	831.6	831.6
100	25	11.0	831.6	842.6
100	100	11.3	831.6	842.9

As can be observed from Table 5, as the temperature and pressure increases, the physical exergy increases. However, this is negligible compared to the chemical exergy. Therefore, the standard chemical exergy value of methane is used for the analysis.

Since crude oil is made up of several components, the chemical exergy is calculated using Eq. (44) below from reference (Farajzadeh *et al.*, 2017), i.e.:

$$Ex_{oil}^{ch} = \sum_{i=1}^{n_{sc}} x_i Ex_{psc}^{ch}, \tag{44}$$

where x_i is the mole fraction and Ex_{psc}^{ch} is the chemical exergy of the pseudo-components in the crude oil. Since there are many components present in the crude oil, the heavier components are usually lumped together into one pseudo-component (Farajzadeh *et al.*, 2017). All components with carbon number from C_7 are lumped and their lower heating values (LHV) are then used to calculate the chemical exergy (Farajzadeh *et al.*, 2017). The LHV is calculated using Eq. (45), i.e.:

$$LHV\left[\frac{kJ}{g}\right] = 55.5 - 14.4SG, \tag{45}$$

where SG is the specific gravity expressed as an average SG of the lumped components. The LHV is then used to calculate the chemical exergy of the lumped components using Eq. (46) (Farajzadeh *et al.*, 2017), i.e.:

$$Ex^{ch} = LHV\left(1.04224 + 0.011925\frac{\beta}{\alpha} - \frac{0.042}{\alpha}\right), \tag{46}$$

where α and β are the carbon and hydrogen number respectively assuming that the components have a formula of $C_\alpha H_\beta$. Using an average carbon number of 19 for all C_{7+} fractions of the oil and an average molecular weight of 268 g/mol, the chemical exergy for the lumped components of 12172 kJ/mol is obtained (Farajzadeh *et al.*, 2017).

Table 6 - Composition of a crude oil sample in mole fraction (Farajzadeh et al., 2017) based on (Riazi, 1997)

Component	Composition mol%	M_w g/mol	Specific gravity	Exergy KJ/mol
C_2	0.19	30.07	0.356	1495.0
C_3	1.88	44.10	0.508	2152.8
C_4	4.54	58.12	0.584	2804.2
C_5	6.57	72.15	0.631	3461.3
C_6	8.59	86.18	0.690	4106.0
C7+	79.23	268.20	0.895	12172

Table 6 shows the calculated exergy value of the lumped components - C_{7+} and the standard chemical exergy values of the other components C_2 to C_6. Using Eq. (44), the exergy of oil using

the data provided in Table 6 is calculated to be 10395.33 kJ/mol or 45561.01 kJ/kg (assuming a molecular weight of the components, $\bar{M}_w = \sum x_i M_i = 228$ g/mol) (Farajzadeh *et al.*, 2017).

The chemical exergy of the produced water is assumed to be negligible. In case of DME, the standard chemical exergy of the produced DME obtained from Semelsberger *et al.* (2006) is ~ 30750 kJ/kg.

4.1.3 Work Streams

The work stream consists of all the processes that cost energy i.e. the energy input needed to get oil. These include manufacturing of DME, water treatment, pumping, artificial lift, transport and separation (DME-Oil-Water).

Manufacturing of DME

To calculate the exergy costs of manufacturing DME, natural gas is used as the feed stock for producing DME using the direct production method. The natural gas, which is assumed to be mainly methane is converted to syngas using the steam reforming method and then converted to DME using a one step process with a bi-functional catalyst (Bin *et al.*, 2008; Ptasinski, 2013). The net reaction is shown in Eq. (47), i.e.:

$$3CO + 3H_2 \leftrightarrow CH_3OCH_3 + CO_2. \quad (47)$$

The exergy value is calculated with a model developed by (Bin *et al.*, 2008) using a 200,000 t/year DME production plant. To see details of the calculation including stream flow rates and compositions of DME and other raw materials used here, please refer to (Bin *et al.*, 2008; Ptasinski, 2013). The main raw materials used for the process are methane (90%) and ethane (10%). From (Bin *et al.*, 2008), the known streams of the inputs and products given in kmol/h are converted to kg/h using the molar masses of the inputs and product. Since the exergy values per unit time of the inputs are known, the power in kJ/s and subsequently in MW can be calculated. Table 7 shows the relevant stream flow rates and compositions used for the calculation.

Table 7 - Stream Flow Rates of Feed stocks and Product (Bin et al., 2008; Ptasinski, 2013)

	kmol/h	kg/h	kJ/s	MW
Natural gas for combustion	149.70	2611.22	37609.05	37.61
Natural gas for reforming	937.00	16344.09	235402.01	235.40
Total Gas		18955.31	273011.06	273.01
DME	422.10	19446.15	166500.00	166.50

To calculate the exergy value of manufacturing DME, we divide the power necessary to manufacture DME at a given rate by the stream flow rate of the DME (given in kmol/h and converted to kg/h using the molar mass of DME) (see Table 7). With these two values, the exergy value of manufacturing one kg of DME ~ 30823 kJ/kg is obtained as shown in Table 8.

Table 8 - Overall Exergy Balance of the DME Manufacturing Process (Bin et al., 2008; Ptasinski, 2013)

	MW
Inputs	273.01
Natural Gas for reforming	235.40
Natural Gas for combustion	37.61
Air	0.00
0utputs	166.50
DME	166.50
Electricity	0.00
Exergy Losses	106.60
Internal (Chemical part)	95.60
Internal (Thermal part)	7.10
External	3.90
Exergy DME (kJ/kg)	**30823.59**

Water Treatment

Water needs to be treated (to meet requirements of surface facilities as well as reservoir properties) before it can be mixed with DME and injected into the reservoir. In this case it is assumed that the water source is close to the field, hence neglecting the exergy requirement needed to transport it. There are several technologies used in water treatment ranging from filtration, adsorption methods to multi-stage flash distillation methods (Farajzadeh *et al.*, 2017). For this thesis, however, a membrane technology is used. The main reason for choosing this technology is because it is easy to operate, has high efficiency and consumes low energy (Farajzadeh *et al.*, 2017). For this technology, the energy consumption is 5 kWh/m^3 (18 kJ/kg) (Farajzadeh *et al.*, 2017; Mallevialle *et al.*, 1996). it is assumed that 20% of the water injected is lost.

Pumping

This involves pumping the water into the reservoir. Eq. (48) is used to calculate the power requirement for this operation, i.e.:

$$Pw_{pump} = \frac{\dot{Q}\Delta P}{\eta_{pump}\eta_{driver}\eta_{pp}}, \tag{48}$$

where $\dot{Q}$ is the water injection rate and ΔP the pressure difference between the injection well and the producer. η_{pump}, η_{driver}, η_{pp} represents the pump mechanical efficiency (80%), the efficiency of electrical driver (90%) and the efficiency of the power plant (50%) respectively (Farajzadeh *et al.*, 2017). These efficiencies combined gives an overall efficiency of the pump of 36% (Eftekhari *et al.*, 2012; Farajzadeh *et al.*, 2017).

During pumping, gravity helps in the process and thus, reduces the overall pump power needed during injection. To calculate the power saved due to gravity, Eq. (49) is used, i.e.:

$$Pw_{gravity} = -Q(t)gd\rho_w 1.2, \tag{49}$$

where g is the gravitational constant, d is the depth of the reservoir and ρ_w is the water density (the factor of 1.2 is included to account for the extra density due to the mixture of DME and water). The exergy consumed by pumping is then calculated using Eq. (50), i.e.:

$$Ex_{pump} = (Pw_{pump} + Pw_{gravity})\Delta t. \tag{50}$$

Artificial Lift

To lift the produced oil, it is assumed that an artificial lift is used. The power requirements of the artificial lift is calculated using Eq. (51) below with the energy consumption in Eq. (52), i.e.:

$$Pw_{artificial\ lift} = \frac{Q_{oil+water} g d \left[\left(\frac{V_{oil}}{V_{total}}\rho_o\right) + \left(\frac{V_{water}}{V_{total}}\right)\rho_w\right]}{\eta_{pump}\eta_{driver}\eta_{pp}}, \quad (51)$$

where V_{water} and V_{oil} are the volumes of water and oil produced respectively.

$$Ex_{artificial\ lift} = Pw_{artificial\ lift}\Delta t. \quad (52)$$

Transport

This involves the transport of the crude oil from the field to the refinery. The energy requirement for this is assumed to be ~188 J/kg-km (Farajzadeh *et al.*, 2017) based on (Skone and Gerdes, 2008; Wang, 2008).

Other Processes

Separating the oil from water, gas, DME and further DME separation from gas, well stimulation, gas processing, pigging of pipelines as well as other processes, which are not covered in detailed in this analysis are assumed to consume an additional 10% of the total invested exergy.

4.1.4 Production Cycle

The current production cycle uses the conventional way of producing oil and DME i.e. as is currently the state of the art situation. It is assumed that DME is produced either using the gas produced from the field or from other sources. After production, it is transported to the field (transporting cost not regarded in this analysis) and then used for Enhanced Oil Recovery (EOR). The produced DME is assumed to be reinjected and the produced oil/gas is burned in power plants to generate electricity. Figure 36 shows the overall cycle of the process.

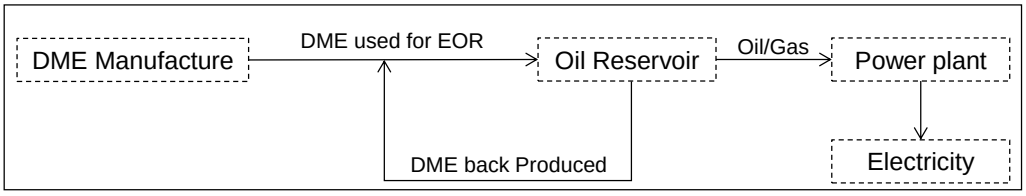

Figure 36 - Current Conventional Method of using DME for Enhanced Water Flood

4.1.5 Exergy Analysis Results and Discussion

Table 9 gives the input parameters and variables used for the exergy calculation.

Table 9 - Summary of Parameters for Exergy Calculation

Parameters	Value	Unit
Water density	1000.0	kg/m^3
DME density at 25^o C	668.0	kg/m^3
Oil density	885.0	kg/m^3
Delta pressure	1.2 x 10^7	Pa
Porosity	0.3	[-]
Exergy of reverse osmosis	18.0	kJ/kg
Oil Exergy	45634.5	kJ/kg
Pump Efficiency	0.36	[-]
Depth	1000.0	m

Parameters	Value	Unit
Oil Transport to Refinery	188.0	J/kg-km
Distance to refinery	500.0	km
Transport exergy	94.0	kJ/kg
CO2 emission (Electricity)	650.0	g CO2/kWh
Other exergy Consumed (% of total energy)	0.1	[-]
DME Exergy	30823.6	kJ/kg

The exergy analysis is done using data from a given field in the Middle East. Figure 37 shows the oil recovery profile (cumulative production), cumulative DME injected and produced.

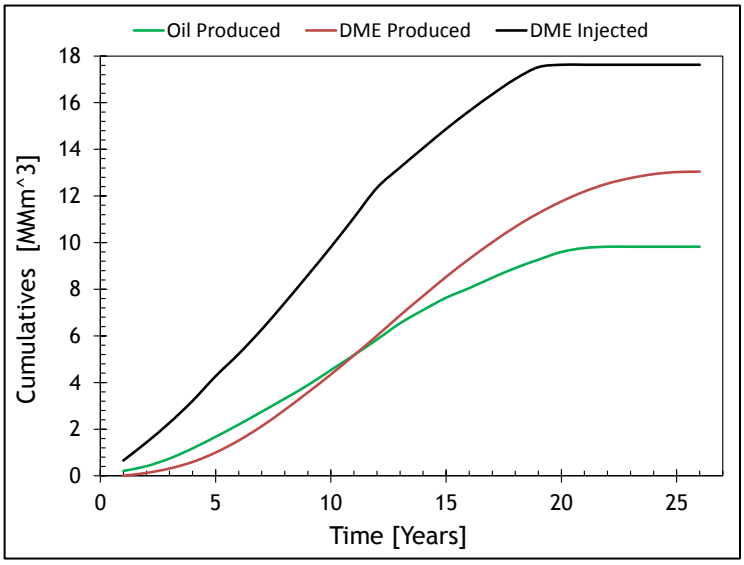

Figure 37 - Cumulative Oil Production, DME Production and DME Injection (Incremental due to DME Injection)

Based on Eq. (41), the Ex_{RF} is calculated using Eq. (53) and considering the system boundary shown in Figure 35.

$$Ex_{RF} = \frac{(Ex_{oil}^{ch} + Ex_{DME}^{Prod}) - (Ex_{DME}^{Manu} + Ex_{pump} + Ex_{treat} + Ex_{lift} + Ex_{others} + Ex_{trans})}{Ex_{oil}^{ch} + Ex_{DME}^{Prod}}, \quad (53)$$

where Ex_{oil}^{ch} is the chemical exergy of the oil produced, Ex_{DME}^{Prod} is the chemical exergy of DME produced, Ex_{DME}^{Manu} is the exergy of manufacturing DME, Ex_{pump} is the exergy of pumping the fluids, Ex_{treat} is the exergy of water treatment, Ex_{lift} is the exergy of lifting the fluids (artificial lift), Ex_{trans} is the exergy of transporting the oil to the refinery from the field and Ex_{others} is the exergy of other processes e.g. separating the oil from water, gas, DME and further DME separation from gas, well stimulation etc.

Figure 38 shows the Ex_{RF} with the parameters listed in Table 9 based on oil production profile in Figure 37. The cumulative exergy recovery factor shows that the process has a negative exergy for the first five years of the project. This is because at the early stage, more DME is being injected than produced. Furthermore, the incremental oil production as of result of injecting DME is low in the first few years (see Appendix G for the mass rates). Since the manufacturing of DME contributes to about 80% (cumulative) (see Figure 39) of the total exergy invested especially in the early stage, this has a significant effect on the overall exergy recovery factor. However, the area above (~20 years) the exergy zero time is more than the one below (5 years). At the end of the project, about 71% of exergy is recovered, with a ~29% loss.

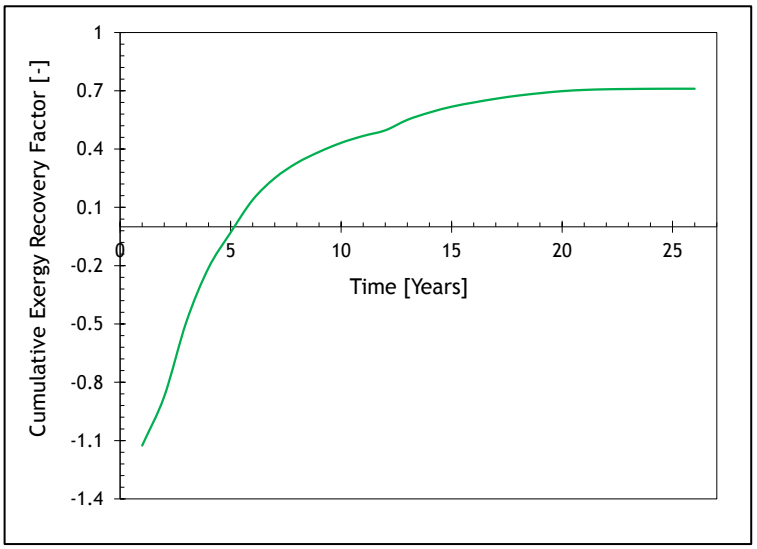

Figure 38 - The Exergy Recovery Factor as a function of Time

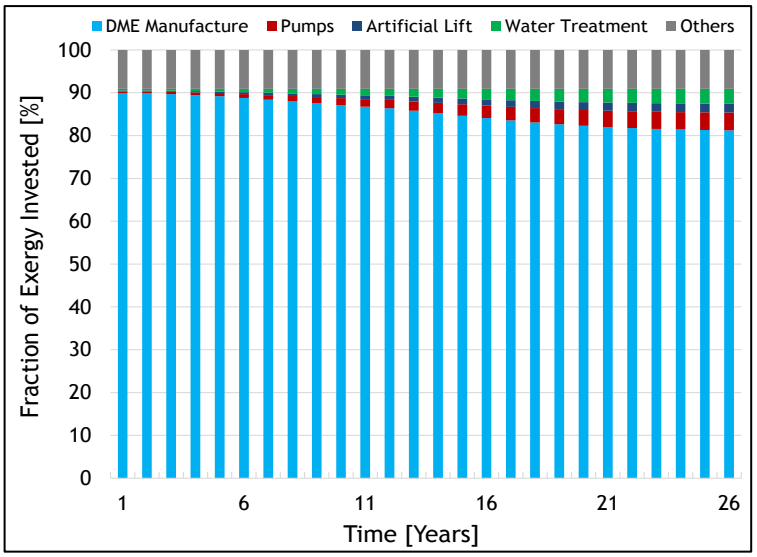

Figure 39 - Fractions of the Invested Exergy in different Components of the Considered System (Cumulative)

Figure 39 shows the fraction of the invested exergy (cumulative) of the different components of the system shown in Figure 35. As is mentioned earlier, the manufacturing of DME contributes to about 90% of the total invested exergy of the overall system. There is a general increase in the exergy related to oil and water. This is because, as time goes by, more oil is produced. Moreover, in order to back produce the DME, more water is pumped into the reservoir, which is why the exergy related to the pump and water treatment also increase progressively.

In order to closely show the effect on DME manufacturing on the exergy recovery factor, the exergy recovery factor rate is plotted against time. This is shown in Figure 40. The three colours: green, red and blue, represent the different stages of the DME injection. In the first stage (the green curve), DME is both manufactured and injected. Until year 3, most of the DME injected is gotten from manufacturing DME i.e. at this time, not much of the DME is being back produced yet. This remains the same until year 5. From year 5, the manufacturing of DME reduces and more than half of the DME needed to be injected is obtained from the back produced DME. This can be seen on the Ex_{RF}. This continues till year 12, where more DME is recovered and reinjected, thereby reducing the exergy invested as a result of manufacturing DME. From year 12 onwards, all of the DME injected is gotten from the recycled DME completely eliminating the exergy of manufacturing DME (see Appendix G). This can be observed in the steep increase in Ex_{RF} – the red curve. The Ex_{RF} stays at about 97% till the end of the red curve. This is because, now more oil and DME are being produced with no exergy consumption as a result of DME

manufacturing. DME injection stops at the beginning of the blue curve leading to less oil and DME production and thus, the Ex_{RF} starts to decrease.

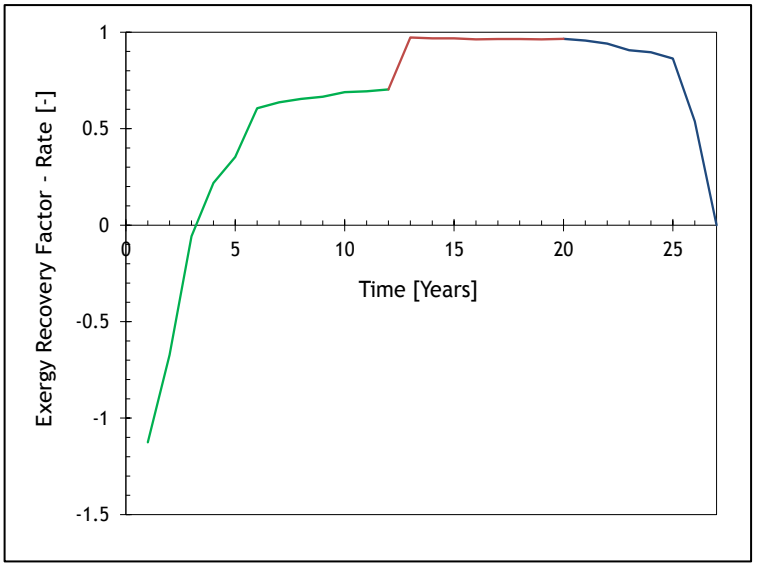

Figure 40 - The Exergy Recovery Factor Rate as a function of Time

Figure 41 shows the fraction of the exergy consumed (rate). DME manufacturing contributes the most to the exergy consumed till year 12, when the manufacturing of DME stops. After this point it can be observed that pumps consumes the most with about 40%. Exergy contribution of transportation is minute and does not have any significant effect on the overall exergy invested.

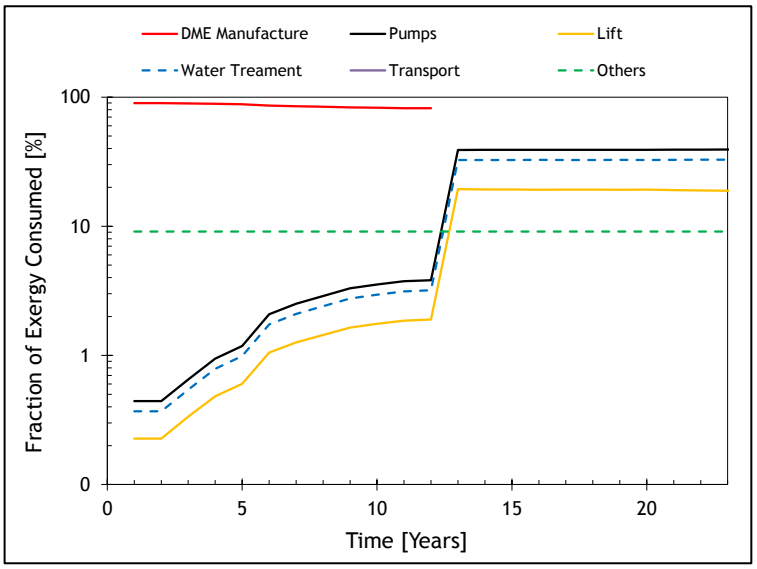

Figure 41 - Fractions of the Consumed Exergy in different Components of the Considered System (Rate)

The manufacturing of DME contributes the most to the exergy invested. A sensitivity of the exergy of manufacturing DME shows a great influence on the exergy lost and recovered at the end of the project. Four cases are looked into i.e. 5000 kJ/kg, 15000 kJ/kg, 25000 kJ/kg and the base case – 30823 kJ/kg and assuming that 20% of the DME injected in lost. All other parameters in Table 9 are kept constant. Figure 42 shows that reducing the exergy of manufacturing DME increases the overall exergy recovered. Moreover, the exergy remains positive for most of the project lifetime as the exergy of manufacturing DME reduces from the base case to the most optimistic case (5000 kJ/kg).

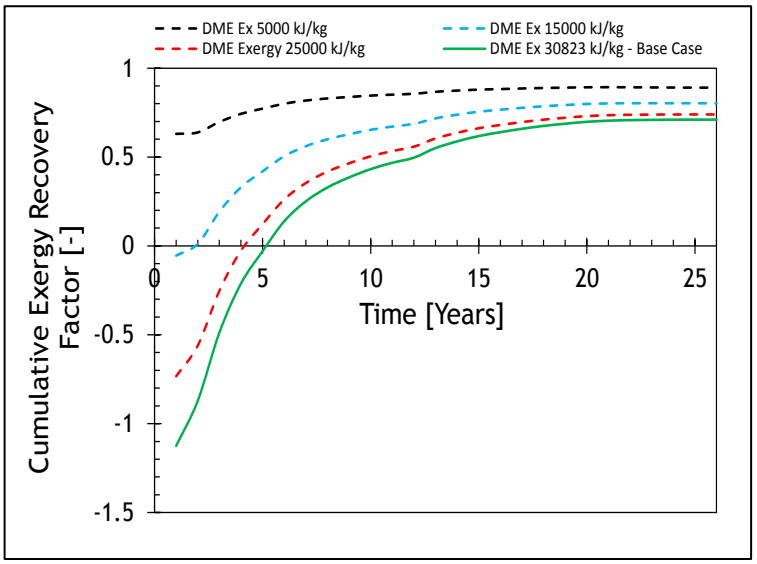

Figure 42 - The Cumulative Exergy Recovery Factor as a function of Time (Sensitivity to Exergy of Manufacturing DME)

The DME utilization factor (ratio of oil produced to the mass of DME injected) also plays a role in how much exergy is recovered at the end of the project. A sensitivity analysis is done on the amount of DME lost to the reservoir. In this case, four scenarios are considered: 10%, 20%, 30% and 40% loss. We assume the same oil and DME production profile as shown in Figure 37. In the base case, it is assumed that 20% of the DME injected is lost. Therefore, 20% more DME has to be injected to produce oil. In the other three scenarios, it is assumed that the oil recovery stays the same. However, in the case of 10% DME loss, the utilization factor increases because less DME is being injected to produce same amount of oil as the base case. In the case of 30% and 40% loss, more DME is injected to compensate for the loss, thus leading to a lower utilization factor (see Appendix H for the profiles of the four different cases). This has an effect on the overall exergy recovery. Figure 43 shows the sensitivity to DME loss to the Ex_{RF}. The Ex_{RF} decreases with increase in DME loss (lower utilization factor).

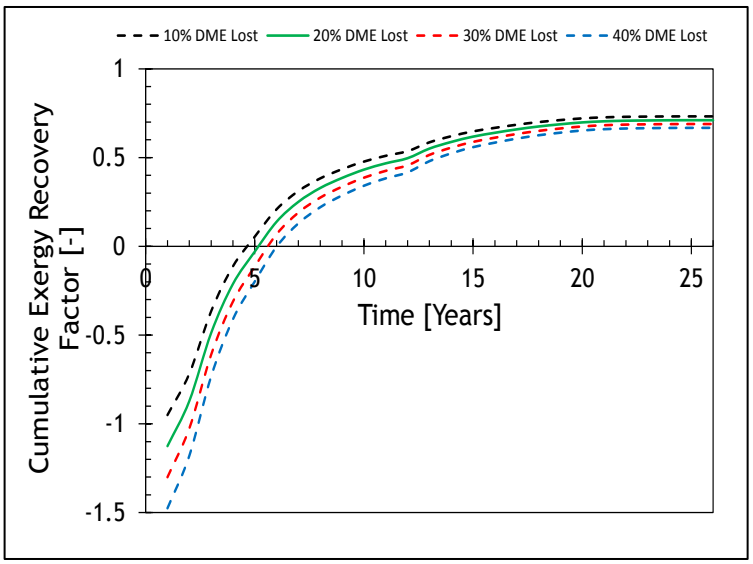

Figure 43 - The Cumulative Exergy Recovery Factor as a function of Time (Sensitivity to DME Lost)

5 DME from Renewable Resources

In Chapter 2, several methods of producing DME are discussed including an innovative method of producing DME from CO_2. This is known as hydrogenation of CO_2 and occurs using the overall reaction in Eq. (54).

$$2CO_2 + 6H_2 \rightarrow CH_3OCH_3 + 3H_2O. \quad (54)$$

The CO_2 used in this process is obtained from power plants. The hydrogen used in the reaction is obtained from water electrolysis. For the method to be renewable, the power source used for the water electrolysis must be renewable (solar, wind or hybrid). Figure 44 shows a schematic of an innovative way of producing DME and its integration into the oil production system. We assume that the oil and gas produced go to power plants. Burning oil and gas to produce electricity releases CO_2, which can be captured and used to produce DME. The DME back produced can either be reinjected in another close-by field or used for other purposes such as electricity generation, methanol production or as replacement fuel for diesel.

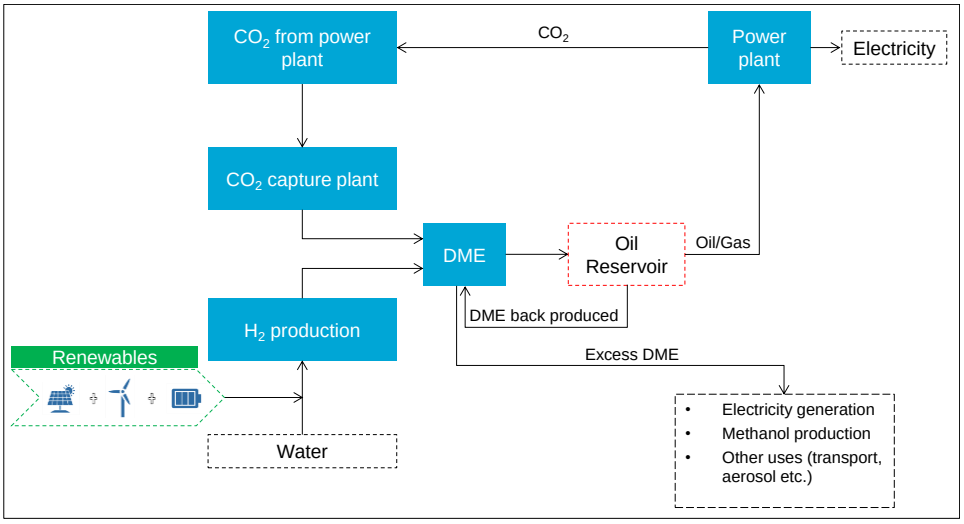

Figure 44 - Innovative Ways of Producing DME and its Integration into the Oil Production System

5.1 Mass Calculations

Not taking into account the method of CO_2 capture, we try to determine how much CO_2 and water (for H_2 production) is needed to produce 1 kg of DME in order to determine the feasibility of the method in meeting the current DME demand based on the field in question. Referring to the net reaction in Eq. (54), 2 moles of CO_2 are needed to produce 1 mole of DME. Thus, using stoichiometric balance, about 1.91 kg of CO_2 is needed to produce 1 kg of DME. In terms of H_2 production, 1.28 kg of water is needed to produce the H_2 needed for 1 kg of DME. Moreover, another 26.8 kg of water is needed to cool the electrolysers used for water electrolysis (Martín, 2016, 2017). Oxygen (O_2) is also produced as a by-product of water electrolysis – 2.1 kg of O_2 produced for every 1 kg of DME.

Using this information, Martín (2016) modelled a scenario using solar PV (photovoltaic) as the source of energy (In Spain) for water electrolysis. Figure 45 shows the monthly production of DME and O_2.

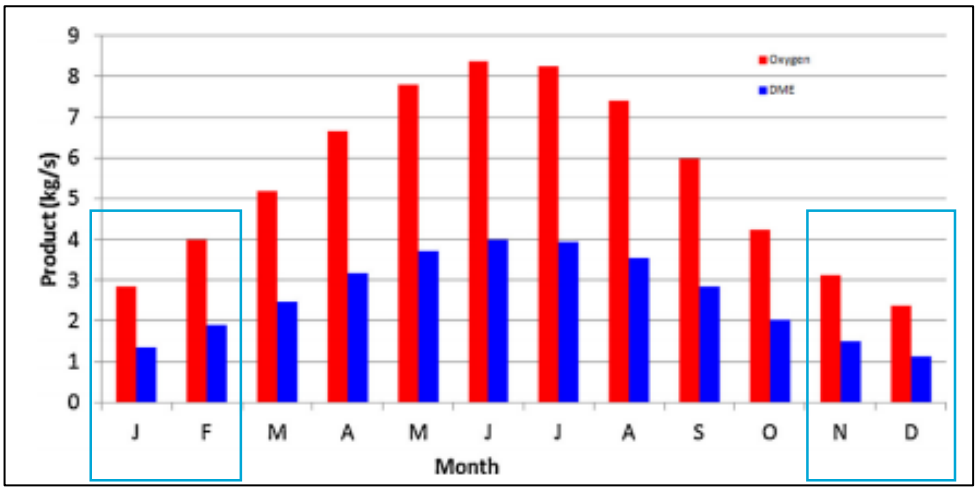

Figure 45 - DME and Oxygen Production (Martín, 2016)

Based on this production cycle, the DME production amounted to an average of 2.64 kg/s, which is about 228 tonnes (t)/day. As can be observed in Figure 45, the production of DME is lower in the winter period mostly due to low solar irradiance (power per unit area of sun received). Notwithstanding this, in those months, the production per day of DME amounts to about 103 t/day. This amounts to an overall capacity of about 82 kilitonnes (kt)/year of DME produced (see Table 10).

Table 10 - Production Summary (Martín, 2016)

	Solar PV
Production Capacity	82 kt/year
Production Cost	1.4 Eur/year
Byproduct (Oxygen)	172 kt/year
CO2 Captured	157 kt/year
Total Water Needed	2307 kt/year
Operation	Seasonal
Energy needed	195 MW

5.2 Renewable Energy Needed

In 2016, there was ~ 2000 GW of installed capacity of renewable energy worldwide with solar and wind accounting for about 40% (Figure 46) (IRENA, 2017). This means that there is a growing trend of installed capacity coming from wind and solar.

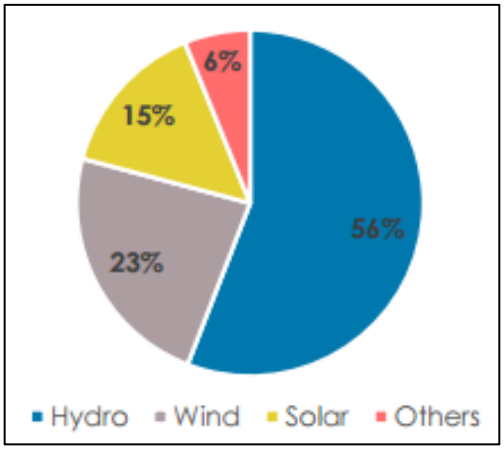

Figure 46 - Share of Renewable Energy (IRENA, 2017)

Solar also saw the highest increase in capacity growth in 2016 (see Figure 47).

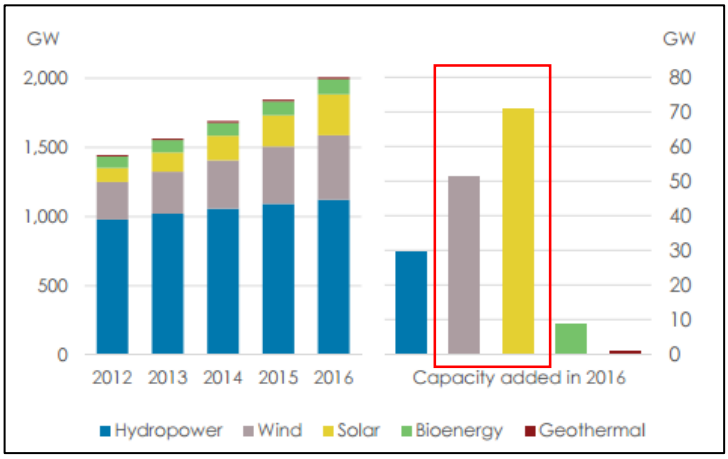

Figure 47 - Capacity Growth (IRENA, 2017)

Moreover, there has been a general increase worldwide in the amount of installed capacity of renewable energy as is shown in Figure 48.

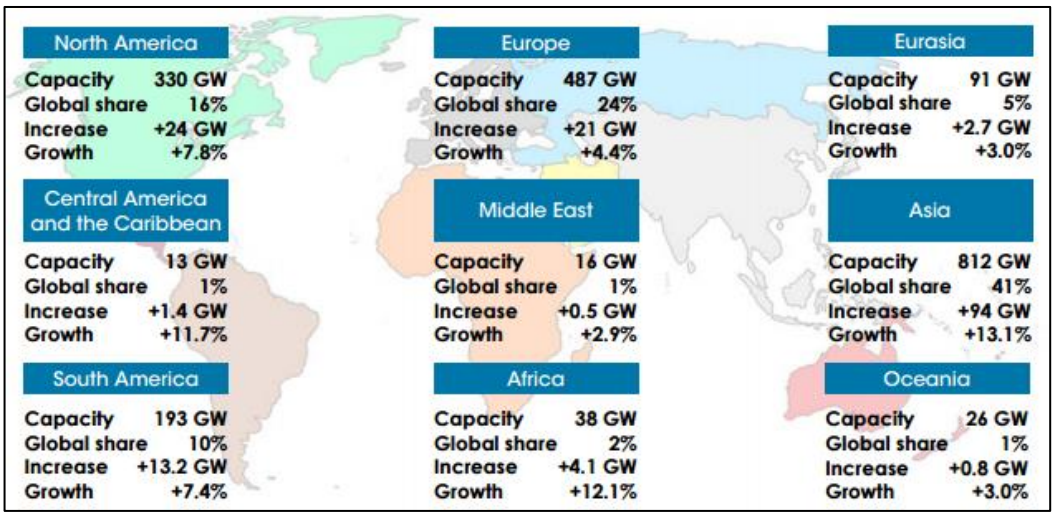

Figure 48 - Installed Capacity of Renewable Energy per Region (IRENA, 2017)

There are however, some limitations to using renewables. The first relates to the inconsistency in supply. Depending on the need, more energy might be needed at times when the sun is not shining or the wind is not blowing. Secondly, though other regions are beginning to catch up in the development of renewable energies, North America, Europe and Asia (mainly China) have been the major players. With vast amount of oil and gas resources in the Middle East and Africa, these regions would have to invest a vast amount of money in renewable energies (especially wind and solar), if there is to be enough installed capacity in these regions to meet the demand needed to produce DME from renewable sources. Other limitations relate to the land needed to install the solar panels or wind turbines.

The solution to solving this problem is location dependent. In the Middle East for example, using solar might be more practical than using wind. And in cases where fluctuation is an issue, solar could be combined with battery storage to meet demand though battery storage technologies are still very expensive at the moment. Another combination could be combining solar and wind in areas that enjoy both good sun shine and moderate wind. Ultimately, the decision of which method to use would depend on the cost and land availability.

5.3 CO_2 Capture

CO_2 can either be captured directly from the atmosphere or from power plants. The first commercial direct CO_2 capture plant was recently developed by Climeworks (Climeworks, 2017). This method has several advantages compared to capturing CO_2 from power plants. One of the advantages is that it is independent of location. This means that the DME plant would not have to be close to a power generating plant. Secondly, about 80% of the energy needed is provided by heat (see Figure 49) (Climeworks, 2017). However, at the moment, it is only possible to produce about 1 kt/year of CO_2 using this method, which is below the amount needed to produce the needed DME.

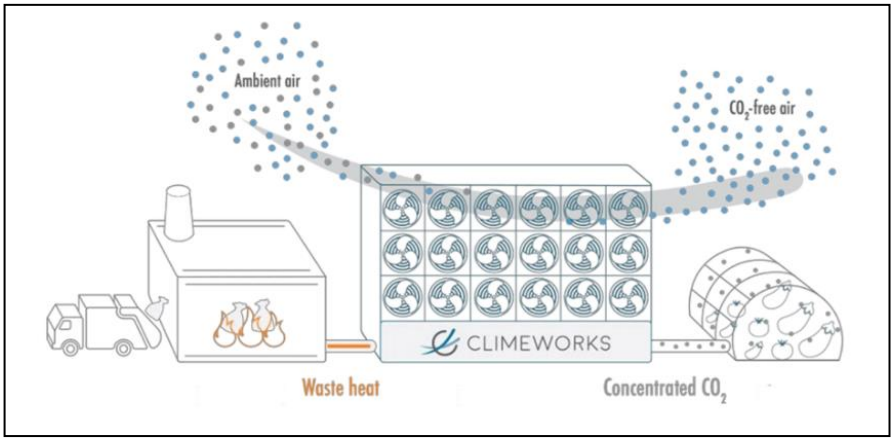

Figure 49 - Climeworks Direct CO_2 Capture Process (Climeworks, 2017)

Other than the direct CO_2 capture from the atmosphere, CO_2 can be captured from power plants, which is a more matured technology compared to direct CO_2 capture. There are currently about 15 large scale Carbon Capture and Storage (CCS) plants worldwide capturing about 27 Mt/year of CO_2, which can be used for Carbon Capture and Utilization (CCU). And there are seven more plants expected to go online in 2018 (IEA, 2015). The disadvantage of this method is that it is location dependent. Since this technology is more established, it is used as the base to calculate the amount of CO_2 released from the power plant assuming that all of the oil and gas produced from the field used in this thesis is burned to generate electricity.

It is assumed that there is an abundant availability of water to produce the hydrogen needed for the DME production.

5.4 DME Production using CO_2 from Power Plants

To determine if the produced oil and gas from the field can generate the required CO_2 needed for DME production, it is assumed that all the oil and gas produced from field are burned in a power plant, which releases a certain amount of CO_2 (see Figure 50). Solar PV is chosen as the preferred source of energy for water electrolysis.

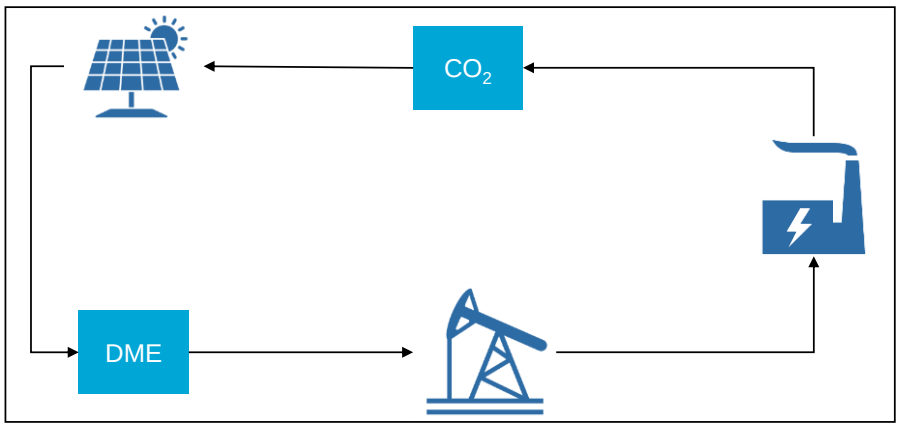

Figure 50 – CO_2 Production from Power Plants

The amount of CO_2 generated by burning oil and gas is calculated using a stoichiometric balance. Oil is assumed to be CH_2 and gas to be CH_4. Eqs. (55) and (56) show combustion reactions for oil and gas respectively.

$$2CH_2 + 3O_2 \rightarrow 2CO_2 + 2H_2O. \quad (55)$$

$$CH_4 + 2O_2 \rightarrow CO_2 + 2H_2O. \quad (56)$$

From the above reactions, burning 1 kg of CH_2 releases 3.14 kg of CO_2 while burning 1 kg of CH_4 releases 2.7 kg of CO_2. And as mentioned earlier, 1.9 kg of CO_2 is needed to produce 1kg of DME. For this calculation, however, it is assumed that the gas produced from is used to generate the electricity needed in field. The CO_2 emissions related to this is not considered in this analysis.

Oil is considered the main product that is burned in the power plant. Using Eq. (55), burning 1 kg of oil gives 3.14 kg of CO_2. The capturing efficiency is 90% i.e. 10% is leaked to the atmosphere. Furthermore, CO_2 is emitted in the capturing process. To calculate the CO_2 emitted in the process, we assume that 4 MJ/kg exergy is needed to capture the CO_2 from the power plant (Eftekhari *et al.*, 2012). Furthermore, additional exergy is needed for compression and transportation (~ 1.5 MJ/kg), leading to a specific exergy of ~ 5.5 MJ/kg. Taking the CO_2 emission per unit exergy of oil to be 0.073 kg/MJ (assuming that 90% of the exergy comes from the fuel) and CO_2 emission using electricity of 650 g CO_2/MWh (10% of the exergy comes from the electricity needed in the process), we obtain a value of ~ 0.36 kg CO_2 emitted/kg CO_2 captured. Therefore, combining the amount of CO_2 emitted in the capturing process with the CO_2 released from burning oil (with a 90% efficiency), the amount of CO_2 produced based on how much oil is burned in the power plant is calculated. And since we know that 1.9 kg of CO_2 is needed to produce 1kg of DME, the amount of DME produced ca also be calculated. This is shown in Figure 51.

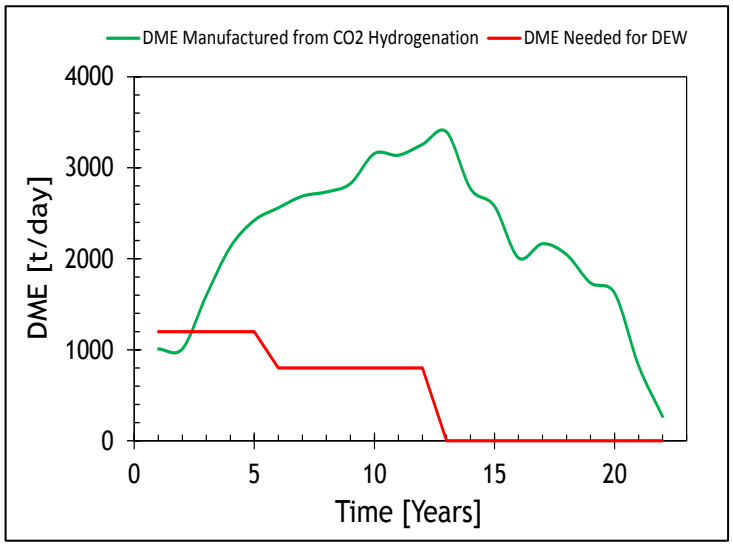

Figure 51 - DME Production and Usage per Day

Figure 51 shows the DME manufactured by using the CO_2 hydrogenation method and the DME needed for DME Enhanced Water-flood (DEW) process. The CO_2 comes from burning the oil from the field. It can be observed that, except for the first two years, there is enough DME to meet the need of the field. The excess DME manufactured can be used in other fields or for other purposes such as electricity generation, methanol production or used for transportation (see Figure 44).

The maximum installed capacity needed to meet the energy requirement to produce the 3400 t/day of DME (Figure 51) is ~ 3GW (assuming that ~200 MW is needed to produce ~230 t/day of DME) – see Figure 45. In 2016, solar and wind accounted for ~ 40% of the 2000 GW installed capacity from renewables i.e. about 800 GW from wind and solar (see Figure 46). 3 GW is about 0.4% of this overall capacity. Considering the growth of wind and solar energy across the globe (Figure 48), there is a high possibility that this can be achieved.

Zooming a bit further into the Middle East where there is abundance of sunlight, there has been an increase in investment in solar PV over the past years and this is expected to grow going into the future. At moment, however, getting ~3 GW of installed capacity from solar alone in the region might be a challenge. Another challenge would be getting this capacity from a single solar farm. Presently, the largest solar farm that is expected to come online in 2019 in the UAE would have an installed capacity of ~ 1.2 GW, which would be the largest solar farm in the world (CleanTechnica, 2017). Though the capacity in the region is expected to increase, the energy requirements would have to be gotten from different solar farms. Figure 52 shows that the region is expected to have about 35 GW of installed capacity from solar PV in 2021 (high case estimate). Moreover, an installed capacity of 3 GW is needed in the case that all of the CO_2 captured would be used to produce DME, leading to an over production than what is actually needed. Depending on the availability, less installed capacity might be needed just to meet the requirements of the field in question i.e. less than 3 GW.

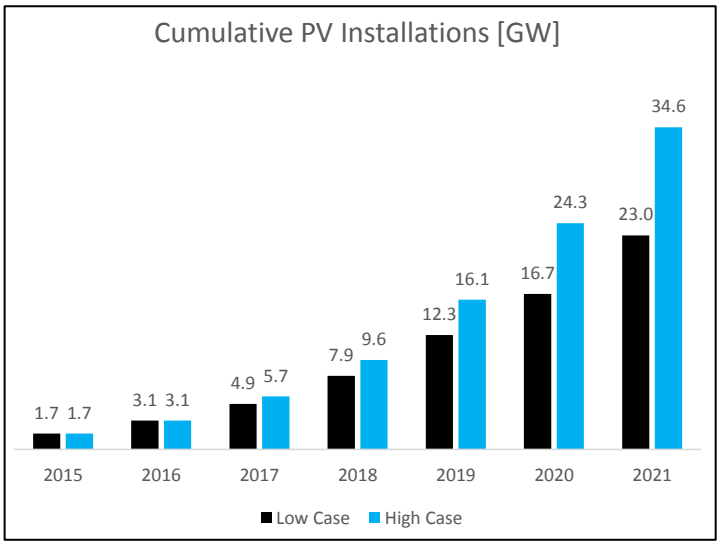

Figure 52 - Cumulative Installation of PV[1] (Apricum, 2017)

In addition to using the excess DME produced for other purposes such as electricity generation and for transportation, CO_2 hydrogenation for DME production has the potential of reducing greenhouse gas (GHG) emissions. Using natural gas to produce DME emits about ~12 g CO_{2eq} /MJ DME[2] (Lee *et al.*, 2016). According to Matzen and Demirel (2016) using CO_2 hydrogenation for DME production has the potential of reducing this GHG emissions by about 82% (using wind energy). This means that this method is cleaner and more sustainable.

[1] Countries included: Algeria, Egypt, Iran, Iraq, Israel, Jordan, Kuwait, Lebanon, Morocco, Oman, Palestine, Qatar, Saudi Arabia, Sudan, Syria, Tunisia, Turkey, UAE, Bahrain, Yemen

[2] Emissions from natural gas recovery, processing and transportation to DME plant not considered

6 Conclusions

Exergy investment in producing hydrocarbons is a relatively small fraction of the energy of the oil produced; yet it can reduce energy consumption in the order of percentages. In areas of high insolation or high wind speed, it can be considered that part of the exergy required for these purposes can be retrieved from sustainable energy sources. This idea is expected to be more important when applying enhanced oil recovery.

As an example, a solvent (Dimethyl Ether - DME) enhanced water drive recovery is used in this thesis. DME is a chemical solvent that has been proven to be an efficient oil recovery agent. The key of using this technology is the back production and re-use of the solvent. The thesis focuses on improving the understanding of exergy streams involved in solvent (DME) enhanced oil recovery. It uses an exergy balance model and estimates the exergy of various components involved in DME enhanced oil recovery. This helps to determine the exergy recovery factor (Ex_{RF}) and to find the various components that contribute the most to the exergy requirements of the process. In order to understand the process, a numerical model is developed and the equations are solved using the commercial finite element package (COMSOL). Moreover, an innovative method for producing DME is looked into, following the ideas of Olah *et al.* (2009), in there book the methanol economy.

The results of the simulation show that the process is highly phase driven, which means that the accuracy of the model depends to a large extent on the accuracy of the phase behavior of the oil/water/DME system. The model shows that about 92% of the oil in place is recovered using DME, which includes about 30% incremental production after water flooding. Moreover the model assumes that 100% of the DME injected is recovered. The oil recovery factor of 92%, similar to what is reported in literature for a simple 1-D model is achieved as if we were using a DME concentration of 63 mol%, which is about five times more than the experimental solubility of DME ~13 mol% in fresh water. Since only a limited number of experimental data are available in the literature (Chernetsky *et al.*, 2015; Ratnakar *et al.*, 2016a) we use DWSIM a chemical process simulator (Medeiros, 2008) to implement the UNIFAC (UNIQUAC Functional-groups Activity Coefficients) method to calculate the phase behaviour of the water-DME-hexadecane system; unfortunately UNIFAC is not very accurate. All the same, to achieve similar results as those reported in literature, a high aqueous phase DME injection concentration is used.

The exergy concept gives an insight into the DME enhanced water flood (DEW) process for a given field in the Middle East. The results show a negative Ex_{RF} at the beginning until about 3 years. The Ex_{RF} becomes positive when the incremental oil produced increases due to the presence of DME. As time proceeds, more DME is back produced, which leads to less manufacturing costs of DME. The time at which the ERF attains zero is called the exergy zero time. For DME enhanced recovery the initial area below exergy zero time plus the area above the exergy zero time is positive. It is found that at the end of the project, about 71% of the exergy is recovered.

The exergy analysis also helps us to identify the various components that contribute the most to the exergy loss (~29%). DME manufacturing is found to be the most important contributor to the exergy loss, contributing ~80% (cumulative) to the total invested exergy. It shows that reducing the exergy of manufacturing DME increases the Ex_{RF}.

The amount of DME lost in the reservoir affects the Ex_{RF} (albeit less than the exergy of manufacturing DME) because it affects the utilization factor (oil produced divided by DME injected). As DME is lost, more DME must be injected without increasing the oil recovery. Consequently, DME loss reduces the Ex_{RF}.

CO_2 hydrogenation (see also Olah *et al.*, 2009)) is one of the innovative ways of producing DME. The method utilizes CO_2 captured from burning the oil in power plants and uses solar PV (photovoltaic) as the source of energy to produce H_2 from water electrolysis. The results show that the CO_2 captured from the power plant by burning the oil produced from the field can be used to produce more DME than what is needed in the field. The excess DME can be reinjected in the field or used for other purposes such as electricity generation, methanol production or for other uses such as replacing Diesel for transportation. It is also found that using CO_2 hydrogenation has the potential to reduce greenhouse gas emissions by about 82% compared to using a natural gas for DME production, which means the method is cleaner and more sustainable.

7 Recommendations

From this thesis, a better understanding has been developed of the exergy requirements of using Dimethyl Ether (DME) for enhanced oil recovery. The following are recommendations made for future research:

1. Since DME manufacturing is found to be the most important contributor to the exergy loss, a detailed exergy analysis on the manufacturing of DME from CO_2 hydrogenation should be done to see if it is possible to reduce the exergy of manufacturing the solvent from this renewable method as a way of reducing the overall amount of exergy invested in the system.

2. A techno-economic analysis should be carried out to determine the feasibility of producing high amount of DME from CO_2 hydrogenation using renewable energies.

References

Aasberg-Petersen, K., Christensen, T.S., Stub Nielsen, C. and Dybkjær, I. (2003), "Recent developments in autothermal reforming and pre-reforming for synthesis gas production in GTL applications", *Advances in C1 Chemistry in the Year 2002*, Vol. 83 No. 1, pp. 253–261.

Air Liquide (n.d), "METHANOL Methanol and Derivatives - Proven Technologies for Optimal Production", available at: https://www.engineering-airliquide.com/sites/activity_eandc/files/2017/05/09/methanol_and_derivatives_brochure_methanol_150pdi_05-017.pdf (accessed 11 June 2017).

Apricum (2017), "Apricum PV Market Model Q3/2017", available at: https://www.apricum-group.com/market-forecasts/ (accessed 11/28/2017).

Azizi, Z., Rezaeimanesh, M., Tohidian, T. and Rahimpour, M.R. (2014), "Dimethyl ether: A review of technologies and production challenges", *Chemical Engineering and Processing: Process Intensification*, Vol. 82 No. Supplement C, pp. 150–172.

Bin, C., Hongguang, J. and Lin, G. (2008), "System study on natural gas-based polygeneration system of DME and electricity", *International Journal of Energy Research*, Vol. 32 No. 8, pp. 722–734.

BioDME (n.d.), "BioDME Project" (accessed 11/16/2017).

Blom, T., Alvarez, A., Lambert, W.J., Marchesin, D. and Bruining, J. (2016), *Low Salinity Carbonated Waterflooding*.

BP (2017), "BP Energy Outlook", available at: https://www.bp.com/content/dam/bp/pdf/energy-economics/energy-outlook-2017/bp-energy-outlook-2017.pdf (accessed 11 October 2017).

Chahardowli, M. and Bruining, H. (Eds.) (2014), *Modeling of Wettability Alteration during Spontaneous Imbibition of Mutually Soluble Solvents in Mixed Wet Fractured Reservoirs*.

Chernetsky, A., Masalmeh, S., Eikmans, D., Boerrigter, P.M., Fadili, A., Parsons, C.A., Parker, A., Boersma, D.M., Cui, J., Dindoruk, B., te Riele, P.M., Alkindi, A. and Azri, N. (Eds.) (2015), *A Novel Enhanced Oil Recovery Technique: Experimental Results and Modelling Workflow of the DME Enhanced Waterflood Technology*.

CleanTechnica (2017), "The Solar Boom In The Middle East", available at: https://cleantechnica.com/2017/09/19/solar-boom-middle-east/ (accessed 11/28/2017).

Climeworks (2017), "The Direct Air Capture (DAC) Plant", available at: http://www.climeworks.com/ (accessed 11 June 2017).

Dadgar, F., Myrstad, R., Pfeifer, P., Holmen, A. and Venvik, H.J. (2016), "Direct dimethyl ether synthesis from synthesis gas: The influence of methanol dehydration on methanol synthesis reaction", *C1 Catalytic Chemistry*, Vol. 270 No. Supplement C, pp. 76–84.

Eftekhari, A.A., van der Kooi, H. and Bruining, H. (2012), "Exergy analysis of underground coal gasification with simultaneous storage of carbon dioxide", *The 24th International Conference on Efficiency, Cost, Optimization, Simulation and Environmental Impact of Energy, ECOS 2011*, Vol. 45 No. 1, pp. 729–745.

Eftekhari, A.A., Wolf, K.H., Rogut, J. and Bruining, H. (2017), "Energy and exergy analysis of alternating injection of oxygen and steam in the low emission underground gasification of deep thin coal", *Applied Energy*, Vol. 208, pp. 62–71.

Farajzadeh, R., Zaal, C., van den Hoek, P. and Bruining Hans (2017), *Life-cycle assessment of water injection into hydrocarbon reservoirs using exergy concept*.

Finnveden, G. and Östlund, P. (1997), "Exergies of natural resources in life-cycle assessment and other applications", *Energy*, Vol. 22 No. 9, pp. 923–931.

Gatlin, C. and Slobod, R.L. (1960), *The Alcohol Slug Process for Increasing Oil Recovery*, Society of Petroleum Engineers.

Goeppert, A., Czaun, M., Jones, J.-P., Surya Prakash, G.K. and Olah, G.A. (2014), "Recycling of carbon dioxide to methanol and derived products - closing the loop", *Chem. Soc. Rev.*, Vol. 43 No. 23, pp. 7995–8048.

Good, D., Francisco, J., Jain, A. and Wuebbles, D. (1998), "Lifetimes and global warming potentials for dimethyl ether and for fluorinated ethers: CH 3 OCF 3 (E143a), CHF 2 OCHF 2 (E134), CHF 2 OCF 3 (E125)", *Journal of Geophysical Research*, Vol. 103.

Groot, J., Chernetsky, A., te Riele, P.M., Dindoruk, B., Cui, J., Wilson, L.C. and Ratnakar, R. (Eds.) (2016a), *Representation of Phase Behavior and PVT Workflow for DME Enhanced Water-Flooding*.

Groot, J., Eikmans, D., Fadili, A. and Romate, J.E. (Eds.) (2016b), *Field-Scale Modelling and Sensitivity Analysis of DME Enhanced Waterflooding*.

Holm, L.W. and Csaszar, A.K. (1962), "Oil Recovery by Solvents Mutually Soluble in Oil and Water", *SPE-117-PA*.

Hon, G. (1989), "Towards a typology of experimental errors. An epistemological view", *Studies in History and Philosophy of Science Part A*, Vol. 20 No. 4, pp. 469–504.

Hooper, H.H., Michel, S. and M. Prausnitz, J. (1988), "Correlation of liquid-liquid equilibria for some water-organic liquid systems in the region 20-250 °C", *Industrial & Engineering Chemistry Research - IND ENG CHEM RES*, Vol. 27.

IEA (2015), "Carbon Capture and Storage:The solution for deep emissions reductions", available at: https://www.iea.org/publications/freepublications/publication/CarbonCaptureandStorageThesolutionfordeepemissionsreductions.pdf (accessed 11 June 2017).

Inokoshi, O., Ohno, Y., Ogawa, T., Inoue, N. and Tokoeda, N. (Eds.) (2005), *A New DME Production Technology 100tons/day DME Direct Synthesis Demonstration Plant Project*.

IRENA (2017), "Renewable capacity highlights", available at: http://www.irena.org/DocumentDownloads/Publications/RE_stats_highlights_2017.pdf (accessed 11 June 2017).

Japan DME Forum (2011), *DME handbook supplement,* [English ed.], Japan DME Forum, Tokyo.

Kurniawan, T.S., Pertamina, P.T. and Siagian, U.W.R. (Eds.) (2016), *Economic Analysis of Dimethyl Ether Production in Indonesia as Alternative Solution for LPG Demand*.

Lee, U., Han, J., Wang, M., Ward, J., Hicks, E., Goodwin, D., Boudreaux, R., Hanarp, P., Salsing, H., Desai, P., Varenne, E., Klintbom, P., Willems, W., Winkler, S., Maas, H., Kleine, R. de, Hansen, J., Shim, T. and Furusjö, E. (2016), "Well-to-Wheels Emissions of Greenhouse Gases and Air Pollutants of Dimethyl Ether from Natural Gas and Renewable Feedstocks in Comparison with Petroleum Gasoline and Diesel in the United States and Europe", *SAE International Journal of Fuels and Lubricants*, Vol. 9.

Liu, K., Song, C. and Subramani, V. (2010), *Hydrogen and syngas production and purification technologies*, Wiley; AIChE, Hoboken, N.J., [New York].

Liu, Y. and Li, Y. (2015), "An exergy-based evaluation model for the performance of the fossil fuel life cycle", *International Journal of Exergy*, Vol. 17 No. 1, p. 92.

Mallevialle, J., Odendaal, P.E. and Wiesner, M.R. (1996), *Water treatment membrane processes: Joël Mallevialle, Peter E. Odendaal, Mark R. Wiesner*, McGraw-Hill, New York, London.

Martín, M. (2016), "Optimal year-round production of DME from CO2 and water using renewable energy", *Journal of CO2 Utilization*, Vol. 13 No. Supplement C, pp. 105–113.

Martín, M. (2017), "Artificial versus Natural Reuse of CO2 for DME Production: Are We Any Closer?", *Engineering*, Vol. 3 No. 2, pp. 166–170.

Matzen, M. and Demirel, Y. (2016), "Methanol and dimethyl ether from renewable hydrogen and carbon dioxide: Alternative fuels production and life-cycle assessment", *Journal of Cleaner Production*, Vol. 139 No. Supplement C, pp. 1068–1077.

Medeiros, D. (2008), DWSIM, available at: dwsim.inforside.com.br (accessed 11 June 2017).

Muzenda, E. (Ed.) (2013), *From UNIQUAC to modified UNIFAC Dortmund a discussion*.

Ogawa, T., Inoue, N., Shikada, T. and Ohno, Y. (2003), "Direct Dimethyl Ether Synthesis", *Journal of Natural Gas Chemistry*, Vol. 12.

Ohno, Y., Inoue, N., Okuyama, K. and Yajima, T. (Eds.) (2005), *New Clean Fuel DME*.

Olah, G.A. (2013), "Towards Oil Independence Through Renewable Methanol Chemistry", *Angewandte Chemie International Edition*, Vol. 52 No. 1, pp. 104–107.

Olah, G.A., Goeppert, A. and Prakash, G.K.S. (2009), *Beyond oil and gas: The methanol economy / George A. Olah, Alain Goeppert, and G.K. Surya Prakash,* 2nd updated and enlarged ed., Wiley-VCH, Weinheim.

Oliveira Júnior, S.d. (2013), *Exergy: Production, cost and renewability / Silvio de Oliveira Jr, Green energy and technology, 1865-3529*, Springer, London.

Parsons, C., Chernetsky, A., Eikmans, D., te Riele, P., Boersma, D., Sersic, I. and Broos, R. (Eds.) (2016), *Introducing a Novel Enhanced Oil Recovery Technology*.
Peters, E.J. (2012), *Advanced petrophysics,* 1st ed., Live Oak Book Company, Austin TX.
Ptasinski, K.J. (2013), *Efficiency of biomass energy: An exergy approach to biofuels, power, and biorefineries*, AIChE the global home of chemical engineers; Wiley John Wiley & Sons Inc, Hoboken New Jersey.
Querol, E., Gonzalez-Regueral, B. and Perez-Benedito, J.L. (2013), *Practical approach to exergy and thermoeconomic analyses of industrial processes, SpringerBriefs in energy*, Springer, London.
Ratnakar, R., Dindoruk, B. and C. Wilson, L. (2016a), "Phase behavior experiments and PVT modeling of DME-brine-crude oil mixtures based on Huron-Vidal mixing rules for EOR applications", *Fluid Phase Equilibria*, Vol. 434.
Ratnakar, R., Dindoruk, B. and Wilson, L. (2016b), "Experimental investigation of DME–water–crude oil phase behavior and PVT modeling for the application of DME-enhanced waterflooding", *Fuel*, Vol. 182 No. Supplement C, pp. 188–197.
Ratnakar, R., Dindoruk, B. and Wilson, L. (Eds.) (2016c), *Use of DME as an EOR Agent: Experimental and Modeling Study to Capture Interactions of DME, Brine and Crudes at Reservoir Conditions*.
Riazi, M.R. (1997), "A Continuous Model for C 7+ Fraction Characterization of Petroleum Fluids", *Industrial & Engineering Chemistry Research*, Vol. 36 No. 10, pp. 4299–4307.
Rivero, R., Rendon, C. and Monroy, L. (1999), "The Exergy of Crude Oil Mixtures and Petroleum Fractions: Calculation and Application", *International Journal of Thermodynamics*, Vol. 2 No. 3.
Roussière, T.L. (2013), "Catalytic Reforming of Methane in the Presence of CO2 and H2O at High Pressure", Ph.D, TU Karlsruhe, Karlsruhe, 2013.
Sankaranarayanan, K., Swaan Arons, J.d. and van der Kooi, H. (2010), *Efficiency and sustainability in the energy and chemical industries: Scientific principles and case studies / Krishnan Sankaranarayanan, Hedzer J. van der Kooi, Jakob de Swaan Arons, Green chemistry and chemical engineering,* 2nd ed., CRC Press/Taylor & Francis, Boca Raton, FL.
Santos, B.A.V., Loureiro, J.M., Ribeiro, A.M., Rodrigues, A.E. and Cunha, A.F. (2015), "Methanol production by bi-reforming", *The Canadian Journal of Chemical Engineering*, Vol. 93 No. 3, pp. 510–526.
Semelsberger, T.A., Borup, R.L. and Greene, H.L. (2006), "Dimethyl ether (DME) as an alternative fuel", *Journal of Power Sources*, Vol. 156 No. 2, pp. 497–511.
Skone, T.J. and Gerdes, K. (2008), "Development of baseline data and analysis of life cycle greenhouse gas emissions of petroleum-based fuels", *National Energy Technology Laboratory*.
Smith, J.M., van Ness, H.C. and Abbott, M.M. (2001), *Introduction to chemical engineering thermodynamics, McGraw-Hill chemical engineering series,* 6th ed., McGraw-Hill, Boston.
Szargut, J.M., Morris, D.R. and Steward, F.R. (1988), *Exergy Analysis of Thermal, Chemical and Metallurgical Processes*.
Taber, J.J., Kamath, I. and Reed, R.L. (1961), "Mechanism of Alcohol Displacement of Oil from Porous Media", *SPE-1536-G*.
Taber, J.J. and Meyer, W.K. (1964), "Investigations of Miscible Displacements of Aqueous and Oleic Phases From Porous Media", *SPE-707-PA*.
Taupy, J.-A. (Ed.) (2007), *DME A Clean Fuel For The Future*.
te Riele, P., Parsons, C., Boerrigter, P., Plantenberg, J., Suijkerbuijk, B., Burggraaf, J., Chernetsky, A., Boersma, D. and Broos, R. (Eds.) (2016), *Implementing a Water Soluble Solvent Based Enhanced Oil Recovery Technology - Aspects of Field Development Planning*.
The Ministry of industry, Orkustofnun, Mitsubishi Heavy Industries, Mitsubishi Corporation and Hekla (2010), *A Feasibility Study Report for a DME Project in Iceland*.
The University of California (2015), *California Dimethyl Ether Multimedia Evaluation*, Berkeley.
Thomas, S. (2008), "Enhanced Oil Recovery - An Overview", *Oil & Gas Science and Technology - Revue de l'IFP*, Vol. 63 No. 1, pp. 9–19.
TOYO Engineering Corp (n.d.), "DME (Dimethyl Ether)", available at: http://www.toyo-eng.com/jp/en/products/energy/dme/ (accessed 11 June 2017).

Tuong-Van Nguyen, Brian Elmegaard, Leonardo Pierobon, Fredrik Haglind and Peter Breuhaus (2012), “Modelling and analysis of offshore energy systems on North Sea oil and gas platforms”, in *Proceedings of the 53rd SIMS conference on Simulation and Modelling*.

Voldsund, M. (2014), “Exergy analysis of offshore oil and gas processing”, Doctoral Thesis, NTNU, NTNU, Trondheim, 2014.

Wang, M. (2008), “Greenhouse gases, Regulated Emissions and Energy Use in Transportation (GREET) Model. Version 1.8b”, available at: www.transportation.anl.gov/software/GREET (accessed 11 June 2017).

Zahedi nezhad, M., Rowshanzamir, S. and Eikani, M.H. (2009), “Autothermal reforming of methane to synthesis gas: Modeling and simulation”, *International Journal of Hydrogen Energy*, Vol. 34 No. 3, pp. 1292–1300.

Appendix A - ATR Reactor (Zahedi nezhad *et al.*, 2009)

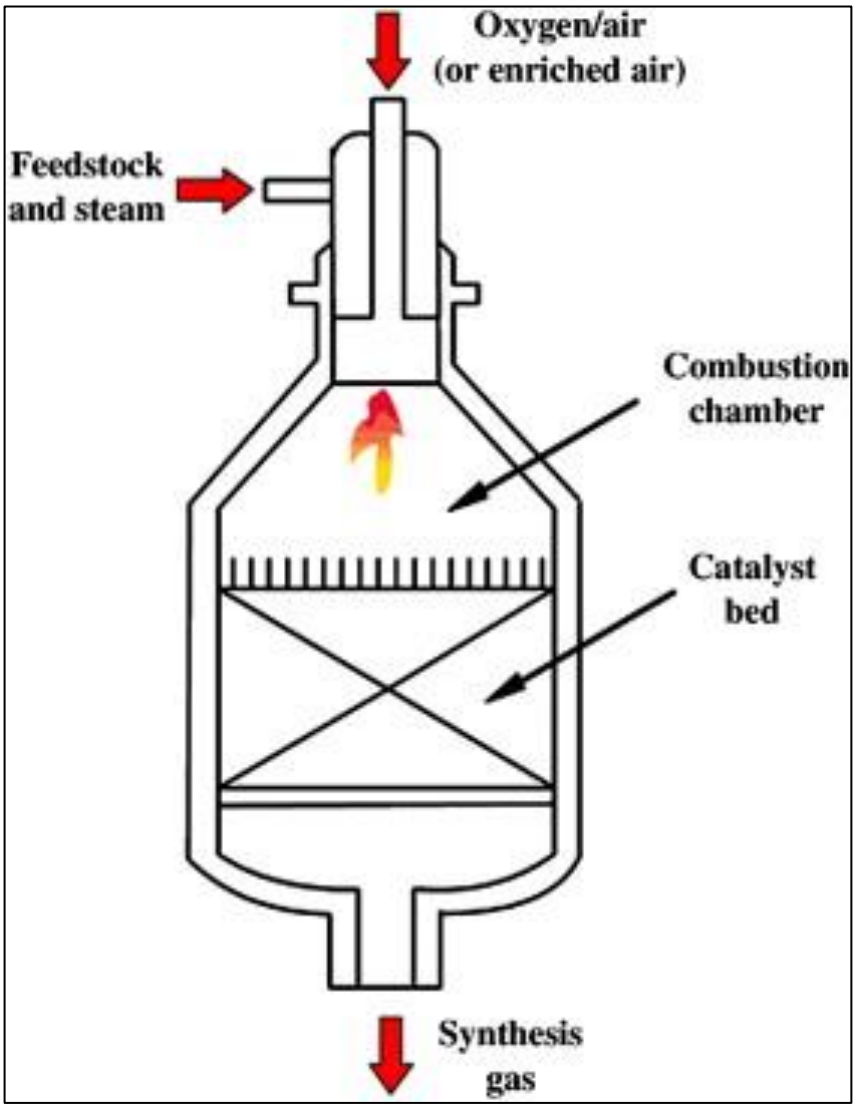

Appendix B - Indirect DME Production using Natural Gas (TOYO Engineering Corp, n.d.)

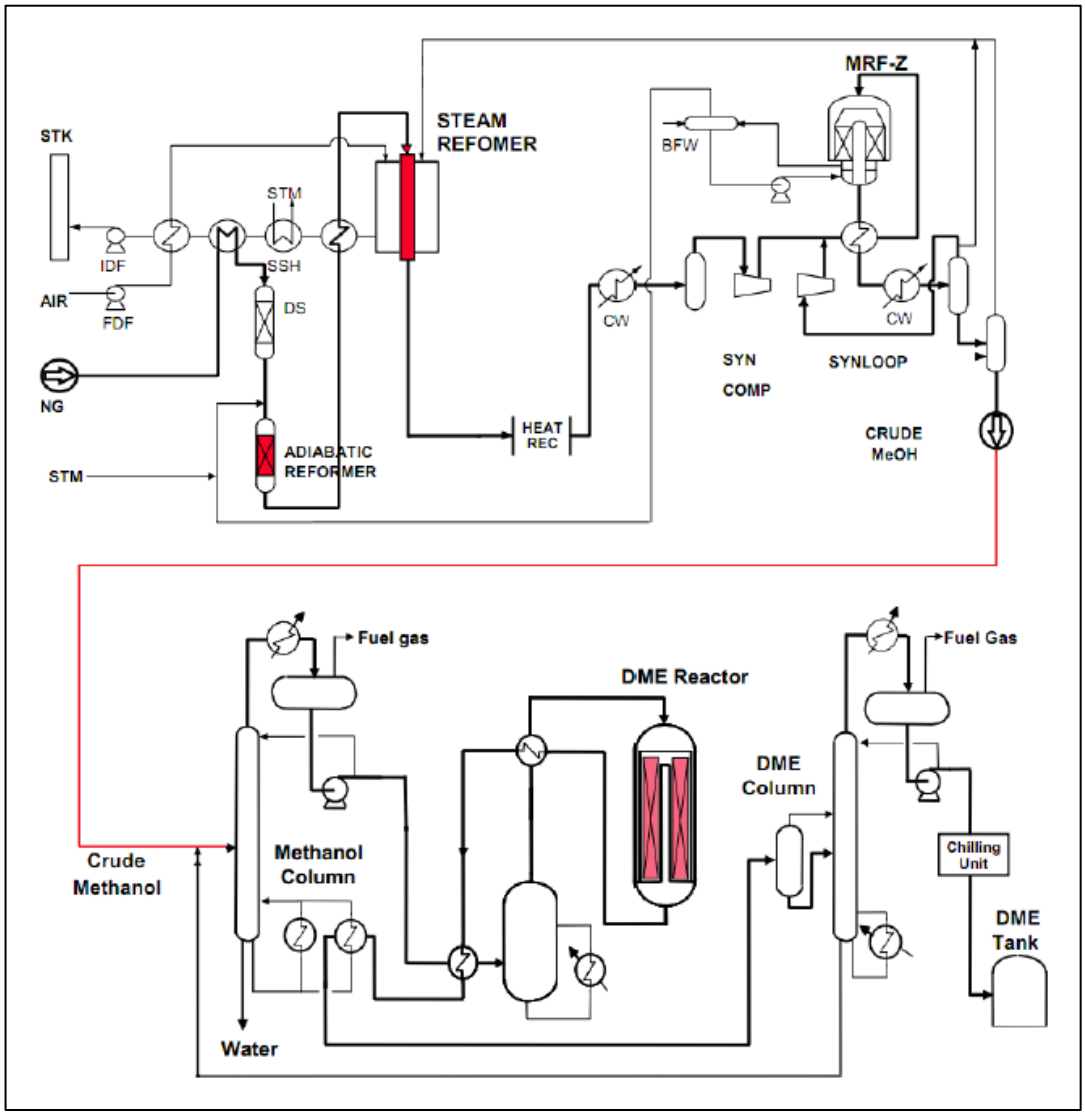

Appendix C - Concept of Slurry Phase DME Reactor (Inokoshi *et al.*, 2005)

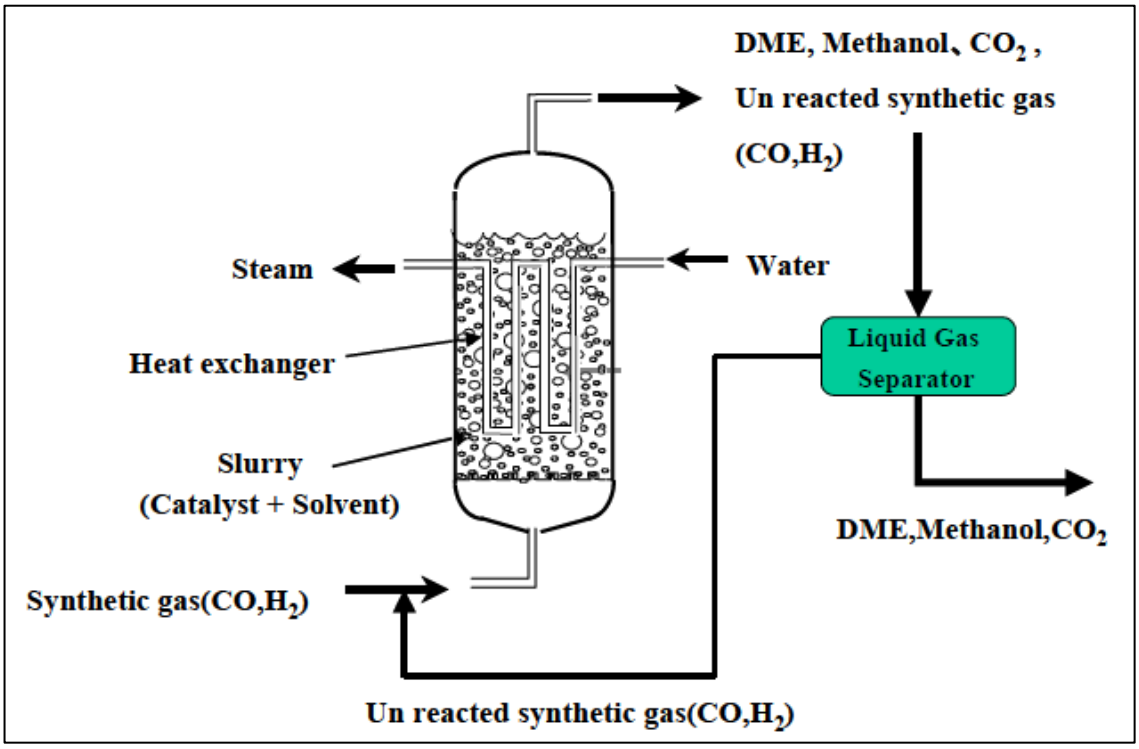

Appendix D - Process Flow of JFE Commercial Demonstration Plant (Inokoshi *et al.*, 2005)

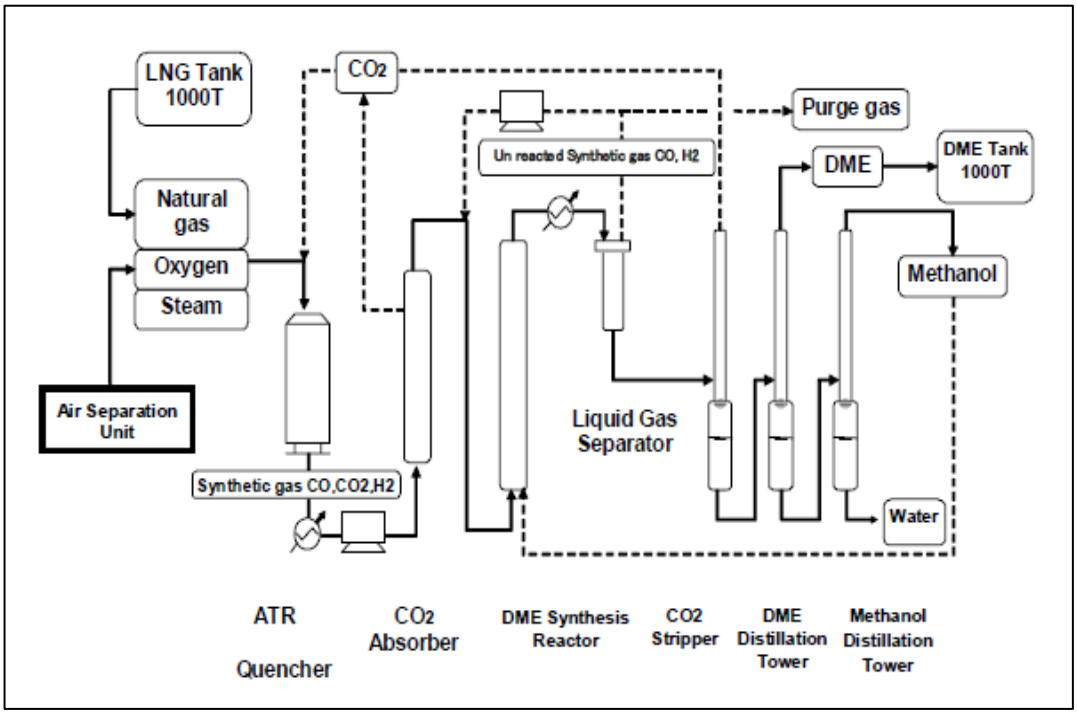

Appendix E - Fractional Flow Curve

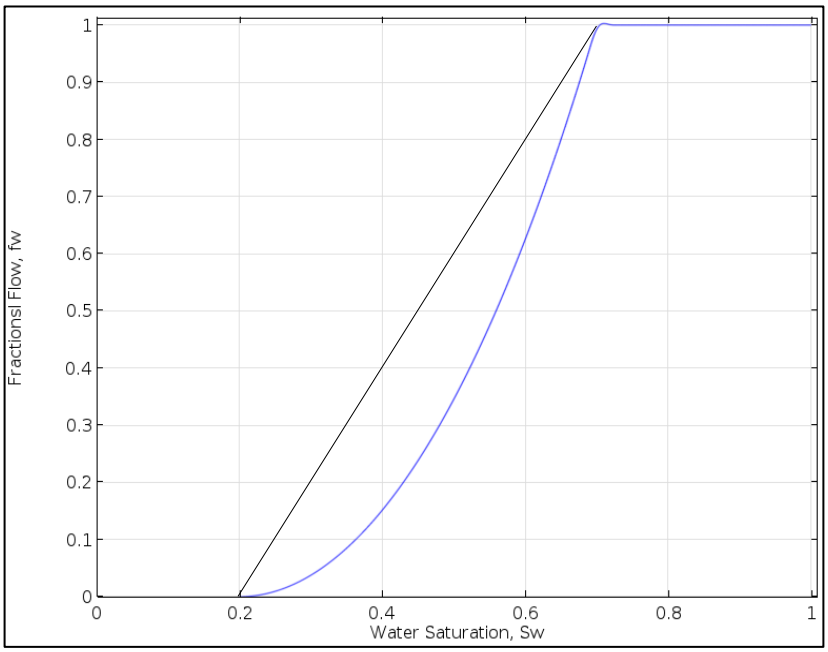

Appendix F - Saturation Profile for Mesh Size 10 m (A), 1 m (B) and 0.1 m (C)

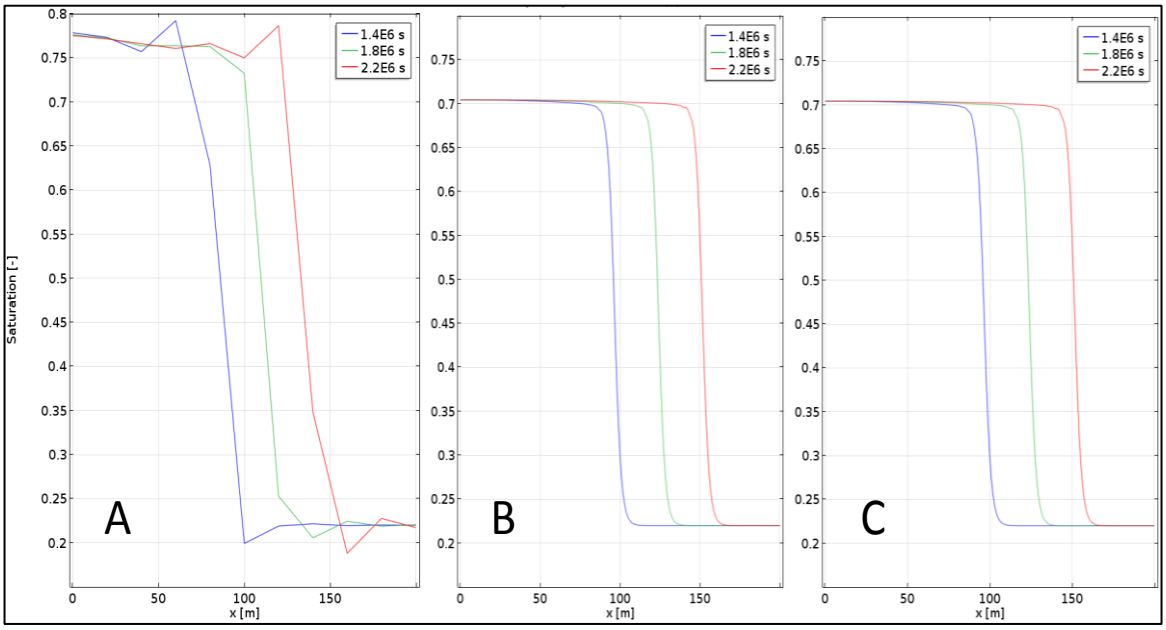

Appendix G - Mass Rates of Oil Production, DME Manufacture, Injection and Production

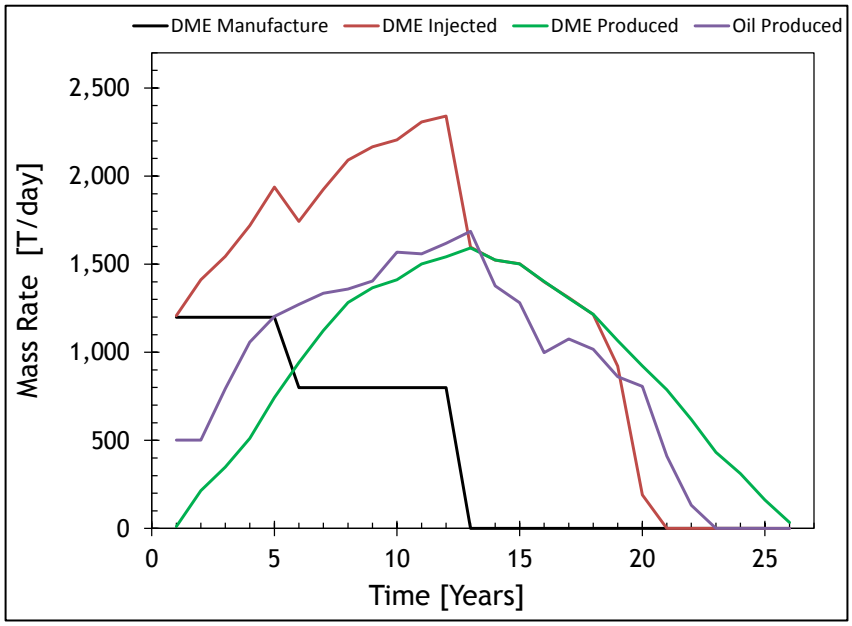

Appendix H - Cumulative DME Injected (4 cases) and Oil/ DME Produced